Role of Co_3O_4 Nanoparticles in Tuning the Dielectric Behavior of CuTI-1223 Superconductor

by

Muhammad Imran

(369-FBAS/MSPHY/F15)

Supervisor

Dr. Muhammad Mumtaz

Assistant Professor

Department of Physics, FBAS,

IIU, Islamabad

Department of Physics

Faculty of Basic and Applied Sciences

International Islamic University H-10, Islamabad

(2017)

i

MS
620.5.
MUR.

Nanotechnology.

Nanoparticles

Polarization.

Nomenclature

Sol gel method

X-Ray diffraction

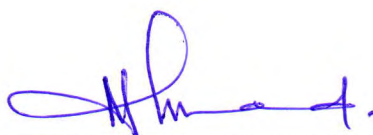# Role of Co_3O_4 Nanoparticles in Tuning the Dielectric Behavior of CuTI-1223 Superconductor

By

Muhammad Imran

(369-FBAS/MSPHY/F15)

This Thesis submitted to Department of Physics International Islamic University
Islamabad for the award of degree of MS Physics

Chairman Department of Physics

International Islamic University H-10, Islamabad.

Dean Faculty of Basic and Applied Sciences

International Islamic University H-10, Islamabad.
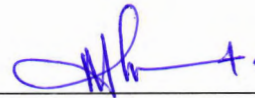
Final Approval

It is certified that the work presented in this thesis titled **"Role of Co$_3$O$_4$ Nanoparticles in Tuning the Dielectric Behavior of CuTI-1223 Superconductor"** by **Muhammad Imran** (Reg. No.369-FBAS/MSPHY/F-15) fulfills the requirement for the award of degree of MS Physics from Department of Physics, International Islamic University Islamabad, Pakistan.

Viva Voice Committee

Chairman (Prof. Dr. Mushtaq Ahmad)

(Department of Physics)

Supervisor (Dr. Muhammad Mumtaz)

External Examiner (Prof. Dr. Zafar Iqbal

Internal Examiner (Prof. Dr. Mushtaq Ahmad)

بِسْمِ اللهِ الرَّحْمٰنِ الرَّحِيمِ

DEDICATED

TO

MY BELOVED PARENTS

AND

RESPECTED TEACHERS.

Declaration of Originality

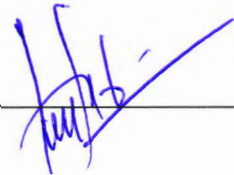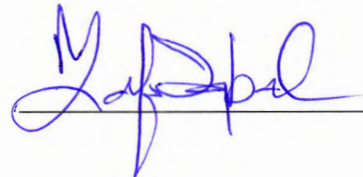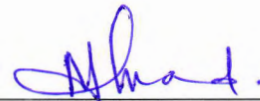I, **Muhammad Imran** Reg. No. 369-FBAS/MSPHY/F-15 student of MS Physics (Session 2015-2017), hereby declare that the work presented in the thesis titled **"Role of Co_3O_4 Nanoparticles in Tuning the Dielectric Behavior of CuTI-1223 Superconductor"** in partial fulfillment of MS degree in Physics from International Islamic University Islamabad, Pakistan, is my own work and has not been published or submitted as research work or thesis in any form in any other university or institute in Pakistan or abroad.

Muhammad Imran

(369-FBAS/MSPHY/F-15)

Dated: 08\08\2017.

Forwarding Sheet by Research Supervisor

The thesis titled **"Role of Co$_3$O$_4$ Nanoparticles in Tuning the Dielectric Behavior of CuTl-1223 Superconductor"** submitted by **Muhammad Imran** (Reg.No.369-FBAS/MSPHY/F-15) in partial fulfillment of MS degree in Physics has been completed under my guidance and supervision. I am satisfied with the quality of his research work and allow him to submit this thesis for further process to graduate with Master of Science degree from Department of Physics, as per International Islamic University Islamabad, Pakistan, rules and regulations.

Dr. Muhammad Mumtaz
Assistant Professor (TTS)
Department of Physics,
International Islamic University,
Islamabad.

Dated: 8/8/2017

<u>Acknowledgement</u>

Contents

List of Figures

Abstract

Cobalt oxide (Co_3O_4) nanoparticles and $Cu_{0.5}Tl_{0.5}Ba_2Ca_2Cu_3O_{10-\delta}$ (CuTl-1223) superconducting phase prepared separately by sol-gel and solid state reaction method respectively. Co_3O_4 nanoparticles were mixed in appropriate ratio in CuTl-1223 to get $(Co_3O_4)_x$/CuTl-1223 with x = 0, 0.5 , 1.0 and 2.0 wt. % nanoparticles-superconductor composites. Different experimental techniques were used for structural and dielectric analysis. XRD spectra showed the structure of host CuTl-1223 matrix remains unaltered after the addition of Co_3O_4 nanoparticles. The superconducting properties of host CuTl-1223 phase [$T_{c\ (R=0)}(K)$] were decreased by the increasing the concentration of the Co_3O_4 nanoparticles. The frequency dependence dielectric parameters of $(Co_3O_4)_x$/CuTl-1223 composites were investigated at various operating temperatures from 78 K to 298 K. The gradually decreasing trend of dielectric parameters and increase in ac-conductivity of host CuTl-1223 matrix was observed by adding contents of Co_3O_4 nanoparticles in host CuTl-1223 matrix.

Chapter No.1   Introduction

1.1 Superconductor and Superconductivity

Superconductivity is a phenomenon in which resistance of material completely vanishes below a certain temperature (called critical temperature T_c) and completely excludes the flux lines from its interior part [1]. Kimberling Onnes discovered the first superconductor in 1911. He was working on the liquefaction of mercury (Hg). He observed that the resistivity of mercury vanish at T=4.2K [2,3]. The second property of superconductivity was discovered by W. Meissner and R. Ochsenfeld in 1933. Magnetic field lines are completely expelled out from the interior part of superconducting material below transition temperature T_c, this expulsion of magnetic field lines is known as Meissner effect [4]. Different theories and models have been used to understand phenomena of superconductivity. In 1957 a macroscopic theory was developed by John Bardeen, Leon Cooper and J. Robert known as BCS theory which more perfectly described the phenomenon of superconductivity by using the concept of cooper pair [5,6]. In 1986 a new class of superconductor known as high temperature superconductor (HTSCs) was discovered by Bednorz and Muller [7].

The most important parameters which determine the superconductivity of a material are critical temperature, critical current density and critical magnetic field.

1.1.1 Critical temperature

The resistivity of some materials vanishes at specific temperature which is known the critical temperature of that material and denoted by T_C material shows superconductivity phenomena below this temperature [8].

1
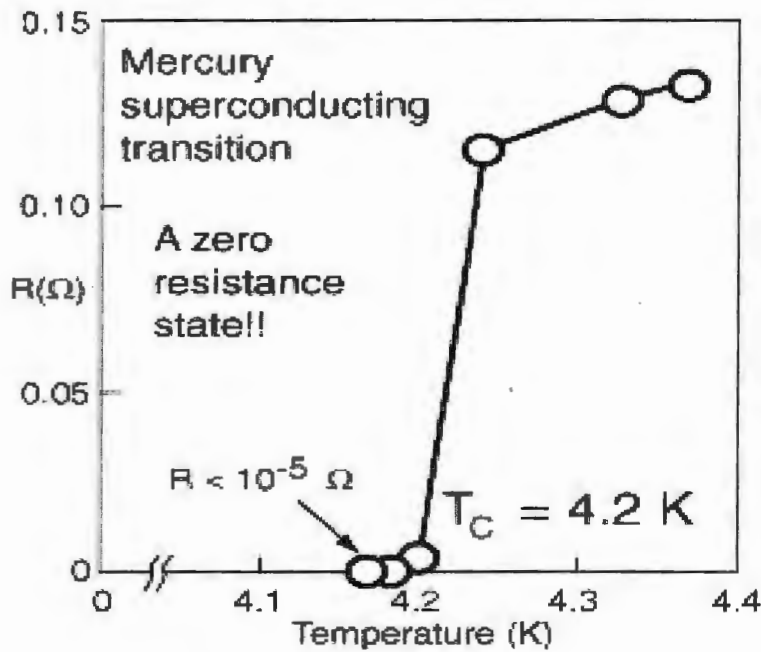
Fig.1.1: Graph b/w temperature and resistance

1.1.2 Critical magnetic field

When superconductor exposed to magnetic field, cooper pair starting breaking as a result superconducting volume fraction start decreasing at specific value of magnetic field and material transforms from superconducting state to normal state, that value of magnetic field is known as critical field H_c of that material [9].
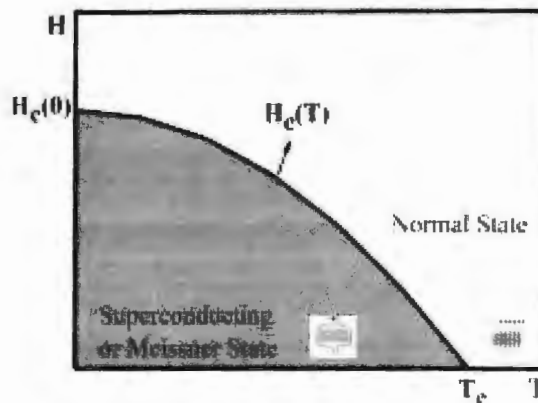
Fig. 1.2: Relationship between superconducting state and H_c

T_c and H_c correlated by given expression.

$$H_c = H_o \left[1 - \left(\frac{T}{T_c} \right)^2 \right] \dots\dots\dots\dots\dots\dots 1.1$$

2

1.1.3 Critical current density

The maximum value of current that a material can transfer without any change of phase from superconducting state to normal state is known as critical current density J_c. The material can transfer current without offering any resistance below the value of J_c and above this limit, the superconductor behave as a normal state [10].

1.1.4 Relationship between superconducting parameters

There are three main factors which define the superconducting phenomenon

- Critical temperature (T_c)
- Critical magnetic field (H_c)
- Critical current density (J_c)

These three parameters define the region in which material behave as a superconductor and above the limit of this region superconducting state transform into normal state. Boundary of superconductor is shown in fig. 1.3.
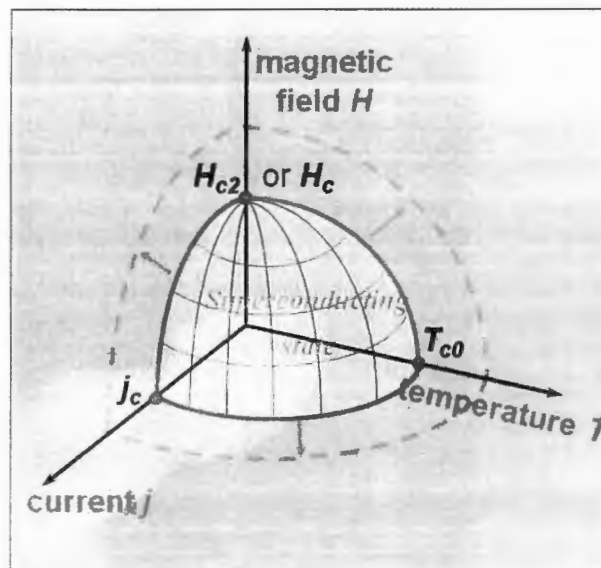
Fig. 1.3: The relationship between H_c, J_c and T_c

1.2 Meissner - Ochsenfeld Effect

In 1933, W. Meissner and R. Ochsenfeld discovered that the superconducting material when cool below T_c and placed in a magnetic field, the field lines are totally excluded, they do not penetrate into the material [11], as shown in fig.1.4.
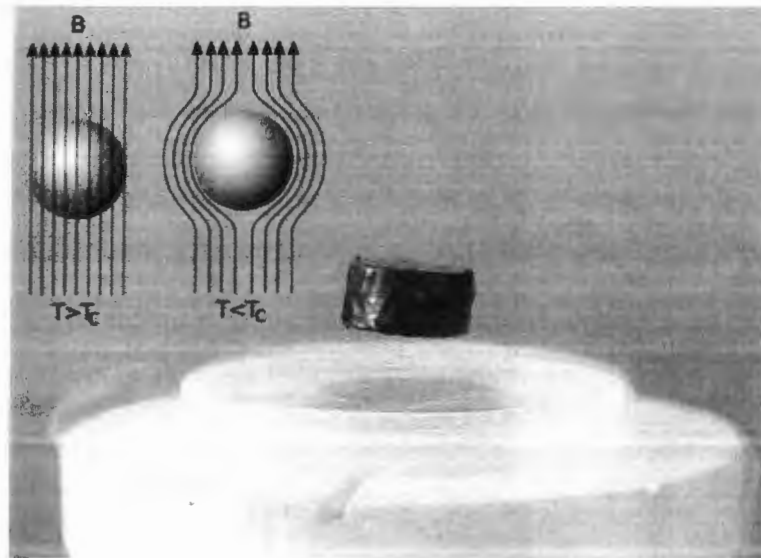
Fig. 1.4: Meissner Effect

1.3 Classifications of Superconductors

In the view of Meissner effect, the response of superconductors to external magnetic field tends to classify superconductors into two types. Type-1 and Type-II superconductors [12].

1.3.1 Type I Superconductors

Type-I superconductors are those superconductors which suddenly losses all of their magnetization and superconducting state, when applied field is greater than the value of critical magnetic field "H_c". Type-1 superconductors are mostly elemental superconductors and known as soft superconductors. Type-I superconductor exhibits complete Meissener effect. No mixed state is present in type-I superconductors, and material remains in superconducting state below H_c and transforms to normal state above H_c [13]. Pure metals like tin and mercury having low value of H_c are also known as type - 1 superconductor. They show perfect diamagnetic behavior due to zero magnetic fields with in the superconductor.
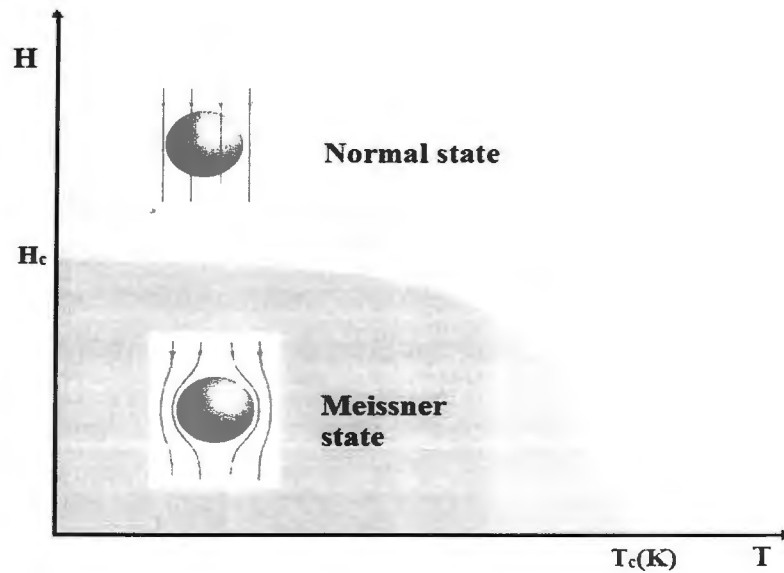
Fig. 1.5: Variation of H_c versus T of type-1 superconductor

1.3.2 Type II Superconductor

Type-II superconductors are those superconductors which gradually lose their magnetization. They have two values of critical magnetic field, lower critical magnetic field H_{c1} and upper critical magnetic field H_{c2}. Three states exist in type-II superconductors i.e. Meissner state, mixed state and normal state. Below H_{c1} materials have Meissner state, between H_{c1} and H_{c2} vortex or mixed state and material transforms to normal state above H_{c2} Type-II superconductors are mostly compound superconductors and also known as hard superconductors [14].
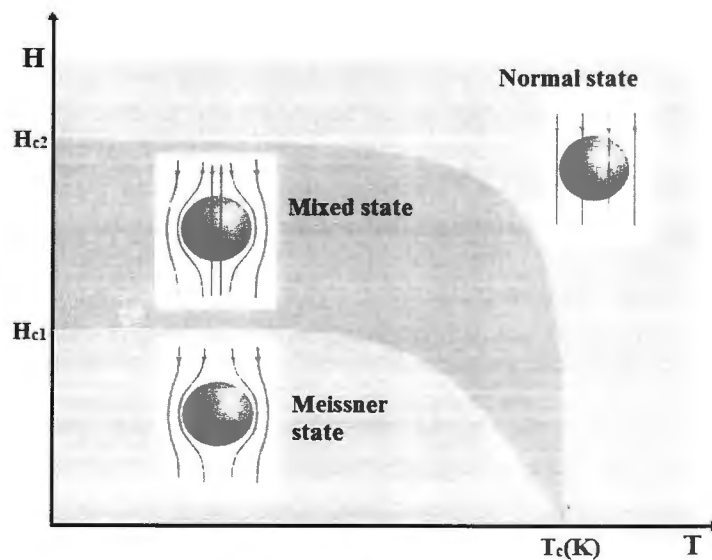
Fig.1.6: Type II superconductors

5

1.4 High Temperature Superconductors

The zero resistivity and little penetration of magnetic lines in some materials are the two most important properties of type-II superconductors. The microscopic origins of these properties are described by BCS theory. The BCS theory tells about the formation of cooper pairs and their coherence length. In low temperature superconductors the coherence length of the cooper pair is larger as compared to the interatomic distance. The coherence length is very small in the high temperature superconductors. The coherence length is $\xi = (1\text{-}2)$ nm for all the high temperature superconductors. However, the coherence length depends upon the anisotropy of the materials [16].

1.5 Nomenclature

The nomenclature of high temperature superconductors are according to IUPAC. There are two parts of HTSC's name. The first part describes the name of composites, usually written in sequence with capital letters. For example, Y-Ba-Cu-O is written as YBCO. The Bi-Sr-Ca-Cu-O stands for BSCCO. The second part tells about the stoichiometry of compound. For example, Y123 stands for $YBa_2Cu_3O_{7-\delta}$, Nd422 is $Nd_4Ba_2Cu_2O_{10-\delta}$, CuTl1223 for $Cu_{0.5}Tl_{0.5}Ba_2Ca_2Cu_3O_{10-\delta}$ [17].

1.5.1 Cuprates

The two series of cuprates compound are Bi-Sr-Ca-Cu-O and Tl-Ba-Ca-Cu-O having the transition temperature between 60K -125K [18]. They have typically orthorhombic and tetragonal structures respectively. The structure of HTSC's cuprates is consist of two layers [18].

- Charge reservoir layer
- Superconducting layer

The superconducting unit cell has two layer structures. The superconducting layer is made of CuO_2 atoms while the charge reservoir layer consists of Tl, Hg, Bi, Cu, and Ba and Sr. these two layers are separated by Ca atoms. The charge carries are supplied by charge reservoir layers to copper oxide layers. When the charge carries passes through the conducting layer, cooper pairs are formed. The cooper pair and their coherence length determine the superconductivity. The critical temperature of superconductor is also determined by number of charge carries in these planes [19-20]. The number of charge reservoir layer and conducting layers has also effect on critical temperature. In case of Tl-Ba-Ca-Cu-O, if we double or triple the layer of Tl_2O_3 the critical temperature increases and if we

increase the CuO_2 layers the critical temperature increases up to n= 3 and decreases with further increase the value of n [21].
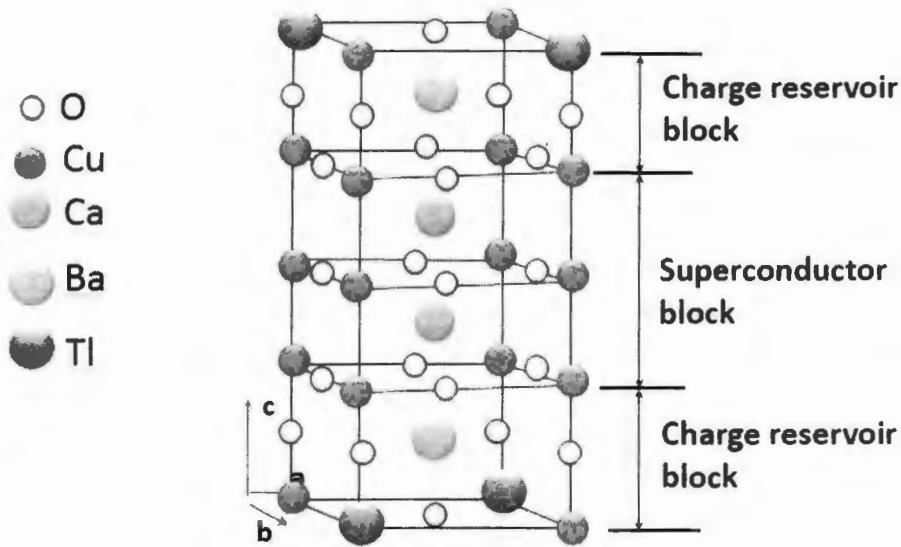
Fig. 1.8: Unit cell of CuTl-1223 superconductor.

1.6 BCS Theory

BCS theory explains the origin of superconductivity. BCS theory was proposed by John Bardeen, Leon cooper and Robert Schrieffer in 1957. According to BCS theory an electron pass through the positively ions carrying definite lattice structure causes a distortion in its shape. When second electron comes than due to phonon, electron lattice attraction dominates over repulsion. Electrons are attracted to each other by phonon than electron pair is called cooper pair. At low temperature cooper pair condensed in ground state of energy level where they behave as bounded pairs of electron. There is a minimum chance of scattering of these electrons pairs so resistivity is zero. Electrons pair behaves as a boson. At high temperature cooper pairs break up and superconductivity disappear [22].
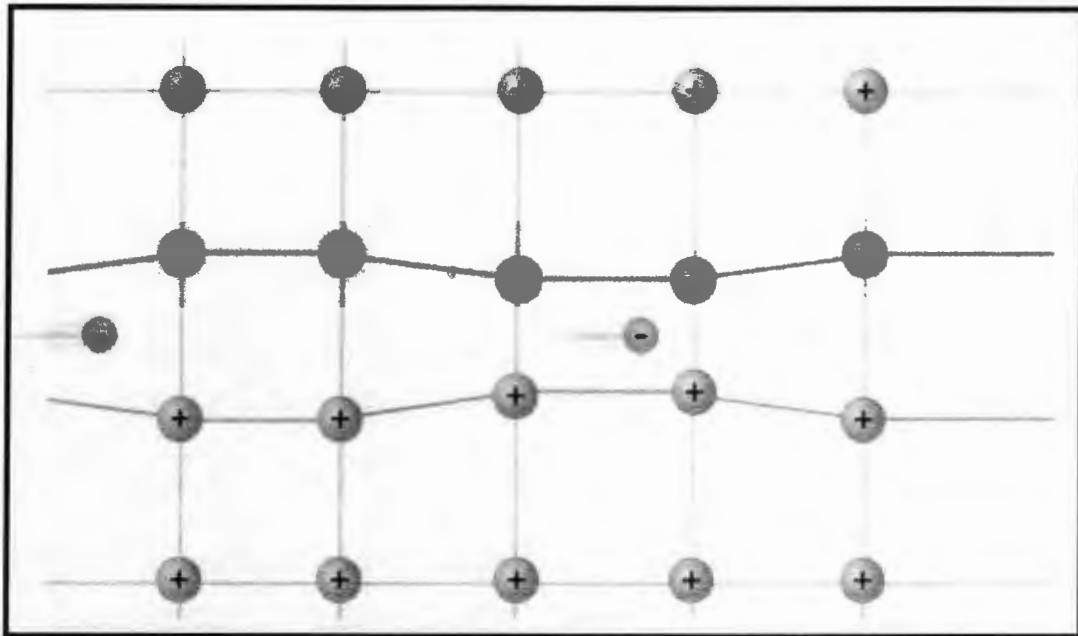
Fig. 1.9: Cooper pair mechanisms in e lattice of superconductor

1.6.1 Coherence Length

In a superconductor there are two layers. One is charge reservoir layer and other is conduction layer where electrons move. BCS theory explains the cooper pair of electrons. When an electron moves through a layer, it distorts the lattice shape and a link is formed with positive ions. When another electron came, it is attracted by ions to form cooper pairs with electron-lattice-electron interaction. These electrons of cooper pair are not fixed. They can move in opposite direction till 10^{-6} m. This length is called coherence length [23].

1.6.2 Penetration Depth

In superconductors, there is a thin layer of electron conduction near the surface of material. When magnetic field is applied it falls into material showing the decreasing trend. But overall it excluded the magnetic field. According to London Equation this magnetic field falls exponentially by increasing the distance into the material.

$$B_{(x)} = B_0 e^{\frac{-x}{\lambda_L}} \dots\dots\dots\dots\dots\dots\dots\dots\dots\dots\dots\dots 1.2$$

This magnetic field penetrate until certain distance λ_L called London penetration depth [24].

1.7   Nanoscience and Nanotechnology

The "nano" is a Greek word stands for minute, petite, tiny, extremely small but in nanotechnology the prefix nano means the one billionth (1×10^{-9}) times smaller than meter. As the size of one atom is about 10^{-15}m while one nanometer is 10^{-9}m, so if 10 Hydrogen atoms or 5 Silicon atoms are aligned each other it becomes nearly one nanometer. Therefore, the study of materials at this scale is known as 'Nanoscience' and therefore functionalizing of those materials is called nanotechnology [25].

1.8   Nanomaterials

Nanomaterials are so small that they can't be seen by a naked eye. At least one dimension of these materials is less than 1 nm. Typically, the nanomaterial's range from (1-100) nm. Nanomaterial's have novel characteristics as compared to normal materials. Nanomaterial's have changed the life style and make the life better [26].Nanomaterials are divided into different types depending upon the structure of materials. They have particle, tube, rod or film like structures. In these different structures the electrons are confined in all or in one, two dimension. On the basis of confinement the nanomaterial's can be classified into three types.

1.8.1 Zero dimensional materials

The materials in which electrons are confined in all three directions are called zero dimensional materials. The dimension ranges size from nanometer to 10 nanometers. The dimensions of materials are smaller than the thermal wavelength of Fermi electrons. The common zero dimension materials are quantum dot or nanoparticles. Zero dimensional materials can be crystalline or amorphous. It can be of different shapes and forms. It can be ceramics, metallic or polymeric [27].
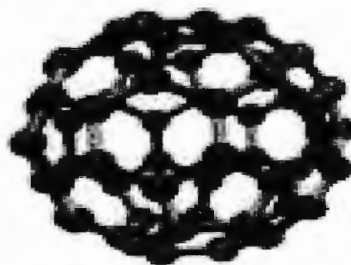
0 D-Fullerene

Fig. 1.10: Zero dimensional material

1.8.2 One dimensional materials

The materials in which electrons are confined in two directions and are allowed to move freely in one direction are called one dimensional material. In one dimensional material, two dimensions ranges are in nanometer range. The common one dimensional material are quantum wire, nanotubes, and nano rods. One dimensional material can be crystalline or amorphous. They may be crystalline or polycrystalline. These materials can be ceramics, polymeric or metallic [28].

Nanotubes,fibers and rods

Fig. 1.11: One dimensional materials

1.8.2 Two dimensional materials

The materials in which electrons are confined in only one direction and allow moving free in two directions are called two dimensional materials. In two dimensional materials one dimension range is in nanometer scale and two can be in micro level. The common two dimensional materials are quantum well, nano films, nano coating, nano layers. Two dimensional materials can be crystalline or amorphous. These particles made up of different chemical compositions, and chemically can be pure or impure. These materials can be ceramics, polymeric or metallic [29].
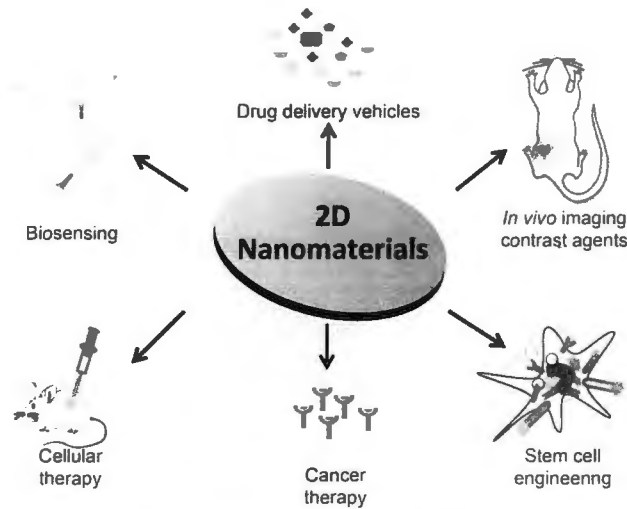
Fig. 1.12: Two dimensional material

1.8.3 Three dimensional materials

In three dimensional materials the motion of electrons is not restricted in any direction or in other word there is no confinement in any direction. The size of these materials is usually larger than 100nm.

1.8.4 Applications of Nanomaterial's

Nanomaterials are produced naturally, but the great interest is taken in engineered nanomaterials. They are used in many products – from the toothpaste to the satellites. These nanomaterials are used from few last years. Due to novel characteristics and some different properties i.e. greater surface area to volume ratio and quantum effects which are usually not presents in bulk materials which changes this world to Nano world. Carbon nanotube is an example that has large flexibility and great strength. In consumer products the nanomaterial's are used, as in cosmetics, sunscreens etc. The nanomaterials are used frequently in many optical and electronic devices. For example normal silicon differs in physical and electronic properties from nanophase silicon, which can be used in macroscopic semiconductor process to make a new better device. In medical sciences the diagnosis and drug deliveries are done by nanomaterial [30]. Some daily use materials which have nanomaterials are

- Hydrophobic cloths
- Car tyres
- Hand soap and shampoo, have zinc oxide nanoparticles
- Anti-scratches eye glass lenses are coated with nanoparticles

11

- Many frictionless lubricants are made
- Zinc oxide nanoparticles are used in sunscreens for the protection from UV light

1.9 Nano crystalline materials

Those particles which have size range from 1 to 100 nm are called nanocrystalline materials. The figure shows some nanocrystalline materials.
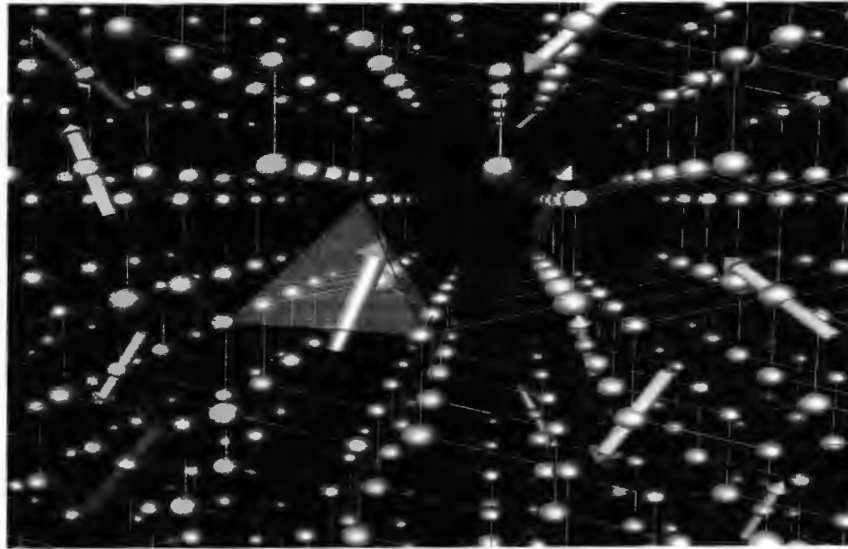
Fig. 1.13: Nanocrystalline materials

They have different properties as compared to their bulk state. They are particularly hard and cannot be broken or smashed. They are strongly reactive. For example, the catalytic properties of silver nanoparticles are different from the bulk silver. In nanoscale the properties change e.g. the conductive material become insulator as we come into nanosize.

1.10   Dielectrics

In a periodic table, there are some elements which conduct electricity by applying external potential difference, such materials are called conductor. But there are some other materials which are poor conductor of electricity such materials are called insulators and also called dielectrics. So a dielectric is an electrical insulator that can be polarized by an applied electric field. Dielectrics are the materials in which energy can be stored by the polarization of molecules. In semiconductors the energy band gap is bit large. In conductors the electrons which are free, moves to opposite direction of applied field. But in insulators microscopic displacements occurs in atoms and molecules.

The insulators are the dielectrics materials and have dielectric constant k which is usually higher than the other materials. Dielectric materials are generally use in capacitors. Dielectric is divided into two types.

- Polar dielectrics
- Non polar dielectrics

Polar dielectrics is found in polar molecules. For example in water is a polar molecule so it has polar dielectrics. In the absence of applied electric field the polar molecules are oriented in random order. When polar molecules are exposed to electric field they tend to align with field in opposite direction.
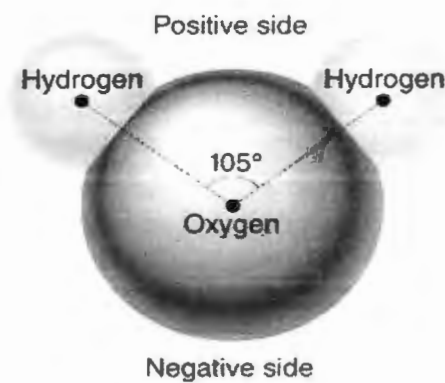
Fig. 1.14: Polar molecules

Although the alignment is not complete, this is due to the random thermal motion. The aligned molecules have an electric field and this field however is smaller than the applied electric field. Whennon-polar dielectrics are exposed to an electric field they form an induced dipole and this dipole moment vanishes in the absence of electric field as shown in fig.1.15

Fig. 1.15: Non polar molecules

1.11 Polarization

"Dipole moment per unit volume" is known as polarization.

Mathematically,

$$P = \frac{\Sigma P}{V} \dots\dots\dots\dots\dots\dots\dots 1.3$$

In the presence of electric field the dielectric becomes polarized. Polarization is either due to atomic, dipolar, ionic and interfacial polarization. fig 1.16 shows the alignment of molecules in the applied electric field and random orientation in the absence of electric field.
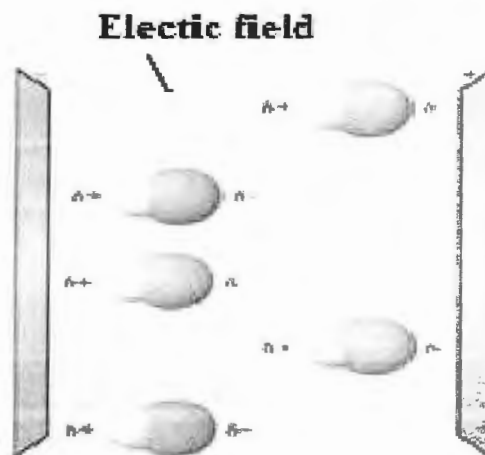
Electic field

Fig. 1.16: polar molecules and its behaviour in applied electric field.

1.12   Types of Polarization

The phenomenon of polarization is observed in dielectric material when the dielectric materials are placed in an electric field and dipole moments are produced in isolated atoms having direction opposite to external field. Therefore the polarization can be defined as the electric dipole moment per unit volume of a dielectric. Polarization is of many kinds depending on the nature of materials such as,

        (a) Atomic polarization

        (b) Dipolar polarization

        (c) Ionic polarization

        (d) Interfacial polarization

1.12.1 Atomic polarization

The atom consists of positively charged nucleus and negative electrons cloud. The atom is completely neutral. When the electric field is applied, its nucleus drifts in one

14

direction and electrons cloud in the other direction. In high electric field the atom ionized but in week field a balance is maintained between the attraction of nucleus, electron and the applied electric field. The molecules polarization depends upon the orientation of molecules and direction of electric field.
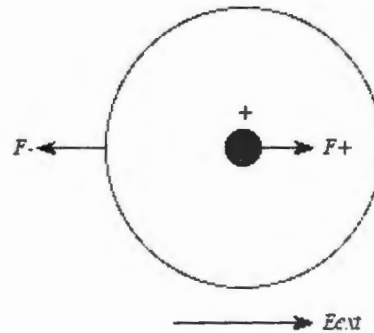
Fig. 1.17: Behaviour of nucleus in presence of electric field E

1.12.2 Dipolar Polarization

Dipolar moment occurs naturally in some materials e.g. H_2O, SiO_2. When an electric field is applied to such materials then its molecules tend to rotate in the direction of electric field. Figure shows that a dipole moment of a molecules experience a torque that align it in the direction of electric field.
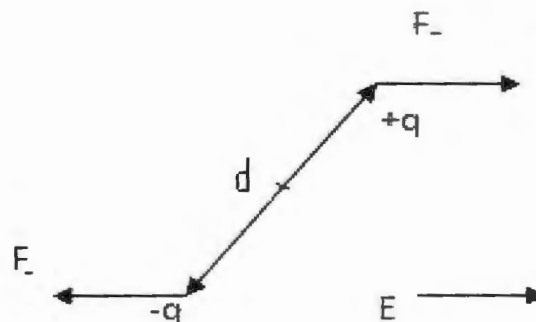
Fig. 1.18: Molecule experiences a force in the direction of E

1.12.3 Ionic polarization

Some dielectric materials have ionic bonding between the atoms. When they are exposed to an electric field a disturbance is produce between the cations and anions and they get aligned in the opposite direction of electric field. This polarization is known as ionic polarization and it is temperature dependent [31].

15
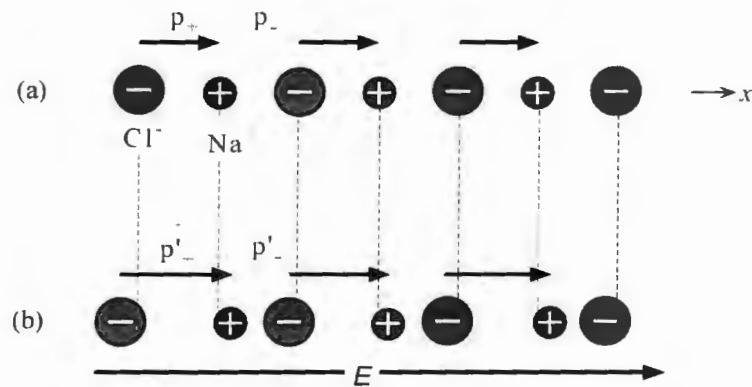
Fig.1.19: The NaCl and displacement in the presence of electric field

1.12.4 Ionic polarization

Some dielectric materials have equal number of fixed negative ion and mobile positive ions. The net dipole moment is zero in the absence of electric field. When an electric field is applied at the electrodes the mobile positive charges will move towards the negative electrode. The negative charges are fixed in the dielectric material whereas their concentration increases at one side. The redistribution of charges in the grain boundaries and interfaces is also taken place and that give rise to interfacial polarization [31]. As shown in fig.1.20.
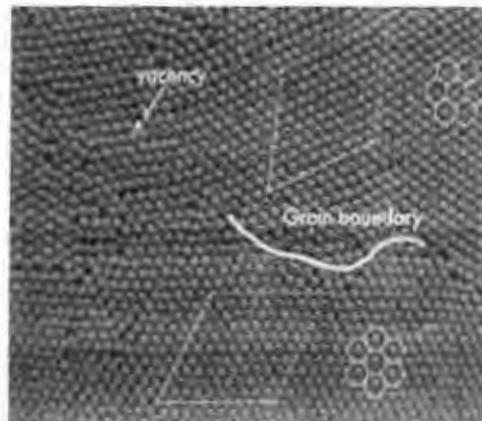
Fig. 1.20: The charged grain boundaries

16

1.13 Dielectric constant

1.13.1 Real part of dielectric constant

When a dielectric medium is placed between the plates of capacitor, the capacitance of capacitors will be

$$C = C_o K_e \dots\dots\dots\dots\dots\dots\dots 1.4$$

Where, K_e is dielectric is constant. For all dielectric constants its value is greater than one. It can also be written as

$$\varepsilon = \varepsilon_o \varepsilon_r \dots\dots\dots\dots\dots\dots\dots 1.5$$

$$\varepsilon_r = \frac{\varepsilon}{\varepsilon_o} \dots\dots\dots\dots\dots\dots\dots 1.6$$

Where, ε is the permittivity of material ε_o is the permittivity in free space, we can also write

$$\varepsilon' = \frac{\varepsilon}{\varepsilon_o} \qquad \dots\dots\dots\dots\dots\dots 1.7$$

ε' is the real part of dielectric constant

1.13.2 Imaginary part of dielectric constant

In an applied electric field the dipoles are tend to align in the direction of electric field. The dipoles oscillate with the alternating field oscillation. If these oscillations are not in phase, this lead to a dielectric loss. In real dielectric part this loss is not shown. So the imaginary part of dielectric is connected to this loss.

$$\varepsilon'' = \varepsilon \tan \delta \dots\dots\dots\dots\dots\dots 1.8$$

The quantity of this loss is expressed as loss tangent [32].

1.13.3 Dielectric loss Tangent

The small phase shift s in the voltage due to presence of dielectric material between plates is known as dielectric loss tangent. There is no phase shift in the absence of dielectric medium [33].
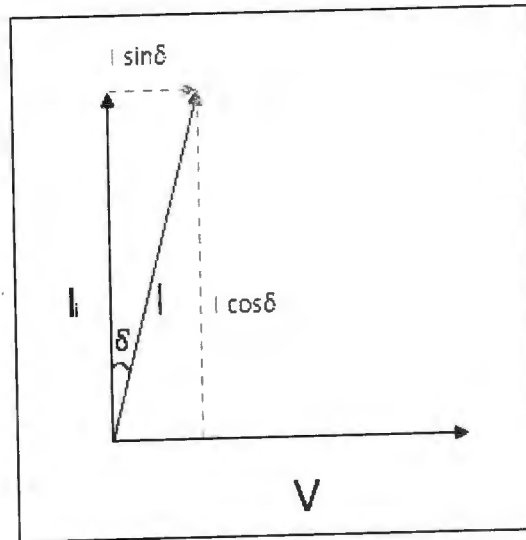
Fig.1.21: Phase shift δ in capacitor due to the dielectric media

It can be calculated by using the formula

$$\tan \delta = \frac{1}{2fRC} \qquad \dots\dots\dots\dots\dots\dots\dots\dots\dots\dots 1.9$$

Chapter 2   Literature Review

2.1 Literature review

S. Cavdar et al [34] examined the Tl based superconductors. Dielectric constant, dielectric loss and conductivity of $Tl_2Ba_2Ca_2Cu_3O_x$ and $Tl_2Ba_2Ca_1Cu_2O_x$ named (Tl-based 223, Tl-based 2212) were observed at frequency range 100 Hz-10 MHz and temperature range 80K-300 K. He observed that dielectric constant, dielectric loss and conductivity were affected by temperature and frequency. In results it was seen that by increasing the frequency, dielectric constant increases and negative capacitance was also observed.

N.H. Mohammad et al [35] studied the dielectric properties of $(Cu_{0.25}Tl_{0.75})$-1234 superconductor with doping MgO nanoparticles in frequency ranges 100 Hz-4MHz and at temperature range from 113 K to 300 K. They observed that real part of dielectric constant increased with doping percentage up to 0.4 wt.%. Which was due to impurities and scattered grain boundaries. But when doping percentage of MgO was increased >0.4 wt.% the real part of dielectric constant decreased because of healing up the micro-cracks and reducing the resistivity by improve the connectivity between grains and grain-boundaries.

M. M. Hassan *et al* [36] synthesized ZnO nanoparticles doped with Fe^{3+} and investigated their dielectric properties. Fe doped ZnO nanoparticles were synthesized by citrate gel method. Five samples were prepared with varying Fe concentration i.e. 0, 3, 5, 7 and 10 % respectively. XRD analysis of these samples revealed that all samples were in single phase possessing hexagonal structure. Frequency range was kept from 75 kHz to 7 MHz. Both the real and imaginary part of dielectric constant decreased with the increase frequency. This is because of the electrons couldn't keep up with the altering E field. The value of dielectric constant decreased with the increasing concentration of Fe.

H.A. Hashem et al [37] investigated the dielectric properties of SnS. Samples were observed in the form of thin film prepared on glass substrate. Dielectric properties were studied at temperature range from 300K-573 K andt frequencies of 1, 10 and 100 KHz. Their dielectric constant, tangent loss and ac conductivity were observed. Results showed that tin sulphide produce partially crystallite in thin film. Activation energies of conduction and relaxation were measured. There was increase in the activation energies according to frequency and thickness.

H. Koraly et al [38] studied the dielectric properties of Bi-2212 superconductor by doping vanadium in frequency range of 10 KHz-10MHz and temperature range of 80K-300K. Values of dielectric constant, dielectric loss and ac conductivity were studied. Small

increase in dielectric constant was observed at high frequency. It was observed that due to doping of vanadium the critical temperature was decreased in sample. Negative capacitance was also observed in samples.

N.A. Khan et al [39] investigated the dielectric parameters of $Cu_{0.5}Tl_{0.5}Ba_2Ca_2Cu_{3-y}Zn_yO_{10-\delta}$ (y=0, 1, 1.5, 2, 2.5). They observed the effects of Zn atoms on the dielectric properties such as dielectric constant, dielectric loss and ac conductivity. They studied the dielectric properties at different temperature and frequency. It was seen that real and imaginary parts of dielectric constant at low frequency 10 KHz were increased by increasing the Zn doping in sample. Ac conductivity was also increased by Zn doping. It was concluded that at high frequency of 10 MHz dielectric polarization arise due to displacement of mobile carriers in ZnO_2/CuO_2 planes of superconductor.

M. Mumtaz et al [40] studied the dielectric related parameters of CuTl-1234 nano-superconductor with frequency from 10 KHz to 10 MHz and temperature from 79 K to 290 K. Negative capacitance was observed in all measurement. Concentration of carriers was observed in the CuO_2 conducting planes, reason for enhancement the dielectric constants and ac conductivity at frequency of 10 KHz. They found resemblance value of the dielectric constants of Tl-2212 and Tl-2223 with dielectric constant of CuTl-1234. They concluded from the results that Tl based superconductors have greater dielectric constants.

Y. Cuy et al [41] examined the dielectric constant of MgB_2 in polycrystalline form at low frequency range 10^3-10^5 Hz. It was observed at temperature from 25 K to 285 K. Calculated value for real and imaginary part of dielectric constant was $>10^7$. It was also noted that by increasing the temperature and electrical conductivity, dielectric constant increases. But at high frequency real part of dielectric constant in depend of frequency.

Alexander Y. Ilyushechkin et al [42] examined the doping effect of MgO nanoparticles in Bi-2212/Ag. They observed that J_c decreased up to doping percentage 4 wt. % due to misalignment of grains. They found that J_c was significantly lower when the thickness of film increases 30 to 40 μm.

M. Farbod et al [43] studied the doping effect of Ag nanoparticles with $YBa_2Cu_3O_{7-\delta}$ bulk superconductor having different Ag sizes and concentrations. It was seen that by increasing Ag doping J_c was also increased. Reason of enhancing the critical current density was due to improvement in connectivity between the grain and grain-boundaries.

M. Mumtaz et al [44] examined the frequency and temperatures dependent dielectric parameters of $Cu_{0.5}Tl_{0.5}Ba_2Ca_2(Cu_{3-y}M_y)O$ (M=Si, Ge, Sn, Y=0,1). At low frequency and temperature negative dielectric constant was observed. They found that Ge doping with

21

sample was cause decrease in dielectric constant. It was due to very high dielectric loss. Ac conductivity also decreased due to Ge doping and Si and Sn doping did not affect the dielectric properties.

The dielectric related parameters as a function of frequency of CuTl-1234 superconductor were examined at various temperatures (78 K to 290 K) and observed the negative capacitance in the material. A typical comparison of dielectric constants of CuTl-1234 with the dielectric constant of Tl-2212 and Tl-2223 were investigated and larger dielectric constant of Tl-based superconductor was observed as compared to CuTl-based superconductors [46].

2.2   Motivation

For application point of view we can tuned the dielectric properties of CuTl-1223 superconductor by

- Varying the contents of Co_3O_4 nanoparticles
- Varying the test frequency
- Varying the operating temperature

Chapter No. 3   Synthesis and Experimental Techniques

3.1 Nano-materials synthesis approaches

There are two approaches for synthesis of nanoparticles

- Top down approach
- Bottom up approach

3.1.1 Top down approach

Top down technique takes bulk materials and form into nanoparticles. There are many top down synthetic methods for the fabrication of nanoparticles such as lithography, ball milling, molding, embossing and skiving etc. These methods are used in many applications. Especially lithography is used in semiconductor industry to form different components of computer chips such as integrated circuits [47].In top down approach commonly used method is lithography. Lithography technique has two types one is photolithography and second is electron beam lithography. In photolithography a thin film is deposited on a substrate and a light sensitive material called photo resist is applied to substrate. A photo-mask is also applied on resist and then ultra violet light is exposed to resist through photo-mask. Chemical bonds are altered in exposed areas and then exposed photo resist is dissolved in liquid developer. After developing an ions beam is bombarded on material to get desired pattern. Photo resist is removed by using annealing process and pattern is formed, which substrate modification completed [48]. In electron beam lithography an electron beam is used on resist in developing instead of ultra violet light.

3.1.2 Bottom up approach

Synthetis of nanomaterials from very basic sized materials from atomic or moleculer species allowing for the precursor particles to grow in size. Some examples of bottom up approaches are chemical vapor deposition(CVD), physical vapor deposition (PVD), moleculer beam epitoxy (MBE), electrochemical depostion (ECD), coprecipitation and sol gel method etc.
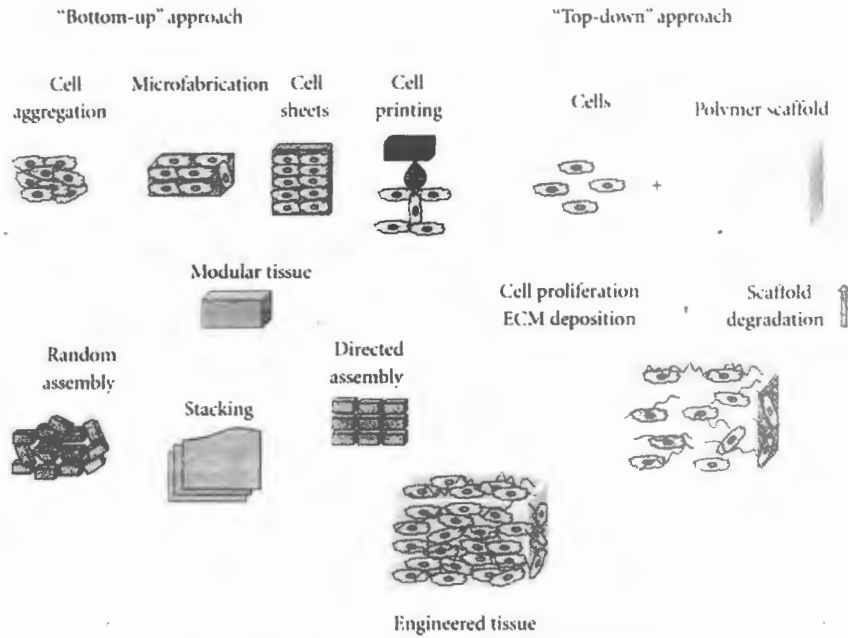
Fig. 3.1: Top down and Bottom up approaches

3.2   Sol gel method

Sol gel is widely used wet chemical technique for the fabrication of nano-materials through a chemical solution, which acts as precursors for a complex network. A sol is basically colloidal suspension of solid or liquid particles ranging from 1-100 nm size and a gel is a colloidal system in which dispersed particles form cross linked networks. Sol gel process has many steps containing mixing, gelation, ageing, drying and firing.
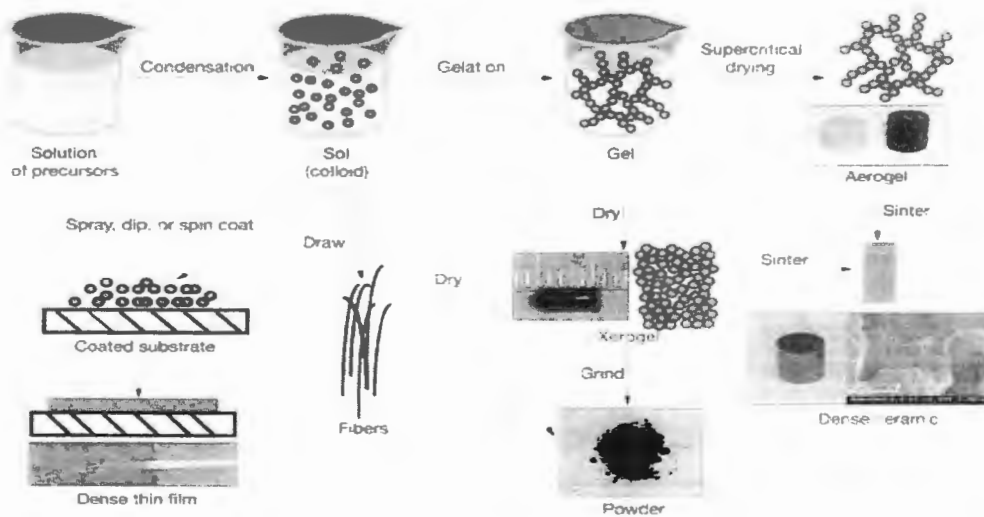
Fig. 3.3: Sol gel process

3.3.1 Mixing

In sol gel process there is a growth of inorganic networks due to the formation of colloidal suspension and gelation of the solution to form gel. Metals are usually used as precursors for the formation of colloids. After mixing compounds in water, two types of processes occurred. One is hydrolysis and other is condensation. Reaction of metal alkoxides MOR with water H_2O undergoes in hydrolysis and condensation stages as

$$MOR+H_2O \rightarrow MOH+ROH \qquad (3.1)$$

$$MOH+ROH \rightarrow M\text{-}O\text{-}M+ROH \qquad (3.2)$$

An example of sol gel method is the formation of silica due to hydrolysis and polymerization of tetraethyl-silicate as in equation 3.3 and 3.4.

$$Si(OCH_2CH_3)_4+H_2O \rightarrow Si(OCH_2CH_3)_3OH+CH_3CH_2OH \qquad (3.3)$$
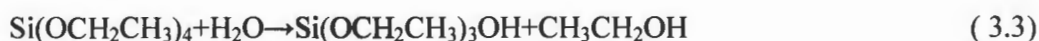
Further hydrolysis and condensation of silanol resulting the formation of two linked silicon atoms through Oxygen Bridge.

$$Si(OCH_2CH_3)_3OH+Si(OCH_2CH_3)_3OH \rightarrow (CH_3CH_2O)_3Si\text{-}O\text{-}Si(OCH_2CH_3)_3+H_2O \quad (3.4)$$

3.2.2 Gelation

Monomers linked to form polymers. Rigidity in the solution of homogenous dispersion cause to form a gel and formation with such process is called gelation. In gelation, inhomogeneity is prohibited. Solution is changed into gel by passing gel point. Sol and gel properties are similar at gel point. Sol is transformed from viscous liquid phase to solid phase at gel point. Gel precipitate gives intermediate state between gel and precipitate [50].

3.2.3 Ageing

Ageing is a continuity of completion of gel process. There is a reinforcing of many extra cross-links in gel structure during ageing process. Gel matrix is contracted and solution is expelled from pores due to ageing process. In ageing process physical properties of gels are changed due to polymerization, phase transformation and coarsening [51]. Sol gel polymerization is observed by changing the catalytic nature, temperature and duration of ageing for different molecular precursors. Ionic and non- ionic catalysts were used in solution. It has been observed that ageing duration has little effect on condensation of atoms of different xero-gel [52].

These are highly volatile due to which it can be purified with ease. Due to mixing the precursors at molecular level solution became very homogenous.

This method is favorable to prepare those materials which are very porous and are nano-crystalline. Acidic and bases based chemical reactions are catalyzed but pH value is maintained to avoid the sensitive organic species such as dyes etc. Biological enzymes are very sensitive to pH. Nanostructures are synthesized with low pressures and temperatures by sol gel method. These nano-materials have less size distribution and high purity [54]. In sol gel method we can obtain materials of different pore size by controlling the ageing and drying process. In this method when liquid state of different materials are cooled down then we can obtain glasses of different materials which cannot be obtained from amorphous solids. Sol gel method is inexpensive

One of the main achievements of sol method is to get the ceramics that may not be prepared from conventional powder processing. There is a resemblance of physical properties of gel derived glasses and those glasses which are obtained from melting. Fibers are prepared with sol gel method from hydrolysis in which continuous fibers are achieved from the solution of metal alkoxide. After ageing and drying process, obtained materials are grinded to get powder form. Powder is further fired to achieve abrasive particles which have very fine grain size <300 nm. Nanoparticles prepared from sol gel method have many applications. Thin film and coating of materials may be achieved from sol gel method.

In coating applications film thickness is very small and drying process is very fast. Four techniques used for coating which are dipping, spinning, lowering and spraying. Antireflection coating, absorbing coating, filters semiconductor coating; protective layers and independent films are prepared by sol gel methods. It is very easy to prepare different kinds of shapes of materials. Sol gel method is very cheap and convenient. Nanoparticles are prepared at low temperature. Sol gel process has very good control on the chemical composition of materials due to which it is used in multi-component materials.

3.3   Solid State Reaction Method

Solid state reaction method may be performed in two ways. One is single step method while other is multi steps method, in order to get Tl based superconductor for our research work. In one step method monoxides are replaced by dioxides. Dioxides are easy to handle and hygroscopic is minimum for this case. For example synthesizing the ZnO particles by one step method, there were also $Zn(OH)_2$ in significant percentage other than ZnO [55]. In one step method mixer powder is directly converted into Tl based superconductor by

calcinations but multi step method has series of calcinations in which sample is heated more than one time.

In solid state method the sample is obtained in consuming more time than some other methods. As $LiMn_{2-x}Co_xO_4$ was prepared from microwave induced method in short time than solid state method [56]. A solid state reaction is performed without solvent therefore; it is also named as solvent-less reaction. In this method two or more solids are mixed and heated. These solids react to form desire products. This method is being used in laboratory and industry. First high temperature superconductors were made by this method. This method is also known as ceramic method [57]. BeB_2 was prepared from solid state reaction and it was seen that below 1.8 K superconductivity vanished [58]. Synthesized BeB_2 was free from impurity component such as unknown phase [59].

3.4 Experimental techniques

3.4.1 Preparation of Co_3O_4 nanoparticles:

Sol gel method was used for the preparation of Co_3O_4 Nanoparticles. 10 gram of cobalt nitrate was mixed in 100 ml distilled water in a beaker considered as first solution and 11.3 g of citric acid was mixed in 60 ml distilled water in separate beaker. For stirring process both solutions after mixing placed on stirrers. To maintain the pH level of solution up to 5 we put ammonia drop by drop to solution. Sample was heated to remove the water from the solution and after some time stirring process stopped and a gel was obtained. To dry the gel we placed in oven for 14 to 16 hours and it was grinded and for annealed in furnace. This sample was again grinded in order to get Co_3O_4 nanoparticles.

Fig. 3.4: Beaker with Magnetic stirring process

3.5.2 Preparation of $(Co_3O_4)_x/$ CuTl-1223 composites

We used solid state reaction method for the synthesis of $Cu_{0.5}Tl_{0.5}Ba_2Cu_3O_{10-\delta}$ superconducting matrix. We used following three compounds as $Ca(NO_3)_2$, $Cu(CN)$ and $Ba(NO_3)_2$. After mixing these compounds, it was grinded and then this mixed material was heated at 860 C^0 for 24 hours and then grinded for 1 hour again, and placed in chamber furnace at temperature at 860 ^0C for 24 hours. It was allowed to cool down at room temperature. Then Tl_2O_3 was mixed with precursor to obtained CuTl-1223. Co_3O_4 nanoparticles powder was added with appropriate wt. % with CuTl-1223 to get five samples with different percentage of Co_3O_4 to obtain $(Co_3O_4)_x/$CuTl-1223 (x=0,0.25,0.5, 1, and 2 wt. %) composites. Powder pressed in hydraulic pressing machine to get pellets with pressure of 3.8 tons/cm^2. These pellets were wrapped into gold capsule and placed into chamber furnace for sintering at 860 C^0 for 10 minutes and allowed to cool at room temperature.

3.6 Characterization Techniques

3.6.1 Crystal diffraction

The building blocks of the crystal lattices are made up of any type of material. These crystals are made by uniform and regular arranged lattices. In lattice, there are three angles of interfacial and lengths of interatomic. Lattices are two dimensional or three dimensional. Uniform and regular arranged lattices make the x-ray diffraction (XRD) peaks during the phenomenon of diffraction.
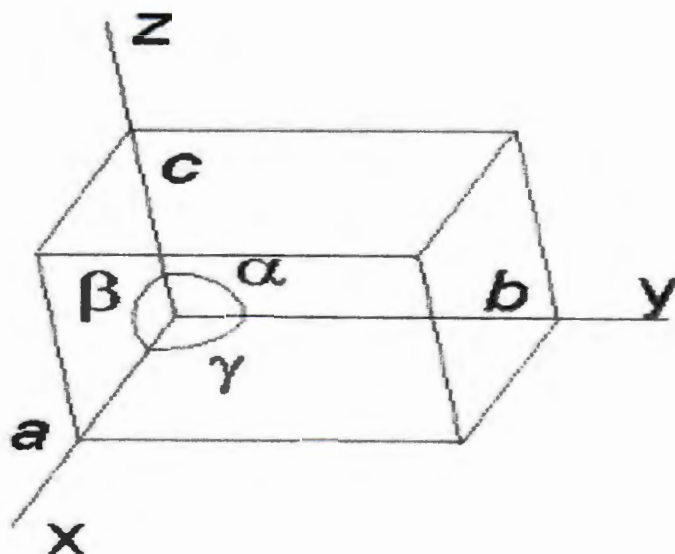
Fig. 3.5: The angles and length of lattice shape

The method of crystal diffraction is used to find out the atomic and molecular arrangement in the crystal. The crystal information is taken when the beam of x-ray of specific wavelength is strike on the surface of crystal and scattered this beam from the crystal. The scattering beams have various information about crystal. The three dimensional pictures got by scientists to observe the relation between light intensity and the angle of scattering from where the beam get scattered. In crystal, the position of the atoms means chemical bonding and other various information of the crystal by the help of this diffracted light.

The materials can naturally occurring are of two types:

- Amorphous materials
- Crystalline materials

The determination of both kinds of materials by the method of diffraction. But we will study is only the crystalline materials. The crystal occurs in the semi-conductor form, metallic form or in the inorganic or organic materials.

A new branch is introduced by scientists called a crystallography, relevant to the crystal structures. The crystallography is the method to find the size of particle. The method of diffraction has been used for the biological applications to observe the proteins, vitamins and DNA like molecules.

The crystal diffraction can find out the arrangement of atoms in the basis of crystal. The crystal diffraction can be produced by various techniques. But we will consider only the x-ray diffraction (XRD) because this technique is relevant to the crystallization of our sample.

3.6.1.1 X-rays

The inner shell (K-shell) electron transitions are the cause of the production of x-rays. The electrons of the outer shell (N-shell) are bound loosely while the electrons of the inner shell (K-shell) are bound tightly around the nucleus. In heavy atoms, the inner shell (K-shell) electron excites and de-excites, to produce a photon, called x-ray. So, the emission of photons beyond the region of ultraviolet electromagnetic radiation due to the inner shell transitions are known as x-rays.

3.6.1.2 Production of x-rays

The x-rays can be generated by the beam of fast moving electrons and strikes on solid incident materials that is tungsten which acts as anode (A). The cooling tube is used for this process. In this process, the production of electrons by the filament (K) acts as cathode. High

voltage is applied between anode and cathode, the emitted electrons are focused into a beam and moved to the incident material. Suddenly decelerated the moving electrons on strike with the incident material, and converting some of its kinetic energy into the x-rays. The x-rays intensity depends upon the current of the filament that is the increase in the number of electrons hitting the incident material, the increase in the intensity of x-rays. The range of the filament current is 100mA to 500mA.

3.6.1.3 X-Ray diffraction (XRD)

The abbreviation of XRD is x-ray diffraction. In 1895, X-ray was discovered by Sir William Rontgen during his experiment of Crooke's tube. The method of X-ray diffraction (XRD) is used to find out the nature of the given material weather the material is crystalline, amorphous or polycrystalline and also used to know the orientation of crystal, crystal size, crystal shape and inter-planer spacing between the layers.
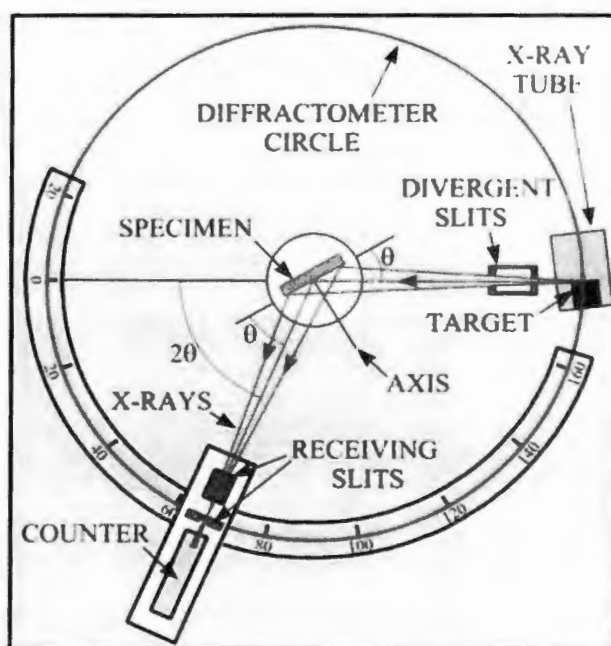
Fig.3.6: Schematic diagram of XRD setup []

In the technique of x-ray diffraction (XRD), on the surface of the crystal, the X-rays beam are strikes on the surface, the reflect beam are interfering with the planes of the atoms before leaving the crystal. In X-ray diffraction technique, we find out the material structure by using the Bragg's law.

31

3.6.1.4   Bragg's Law

In 1912, the Bragg's law was derived by the Physicist Sir William Lawrence. In Physics, the coherent and incoherent angles of scattering from a crystal lattice are given by the Bragg's law. By the help of scattering of electrons, photons or neutrons, we can observe the structure of crystal. This scattering depends upon the wavelength and the crystal structure. In this phenomenon, the radiation wavelengths of neutron waves are relatively similar to the slits width or less than the lattice constant [60].
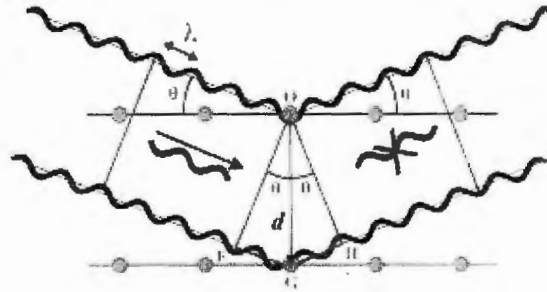
Fig.3.7: Schematic diagram of Bragg's law

In Bragg's law, the interaction of neutron waves scattering emitted from the atomic nuclei with an unpaired electrons. The field of these re-emitted waves either constructively or destructively interferes with each other, and diffraction pattern can be produced on the film. The interference is the cause of these diffraction analysis. Mathematically, Bragg's law can be represented by

$$n\lambda = 2\,d\sin\theta$$

Where, **n** is integer (n = 1, 2, 3, - - - - - - - - -), λ is the wavelength, **d** is the inter-planer spacing in crystal lattice and θ is the angle of scattering.

3.6.1.5 Applications of XRD

- The crystal material can be characterized by the help of X-ray diffraction (XRD).

- XRD, used to characterize the nano-materials as well as bulk materials.

3.7   Scanning Electron Microscope(SEM)

SEM is stand for scanning electron microscope. The SEM can be used for scanning the sample to produce images by the help of focused beam of electrons. The electrons emitted by the electron gun are interacting with the atoms of sample. This focused beam of electrons generating many signals. These signals can be detected by detectors because these signals

have information about the composition of the sample and the surface topography. The scanning of the sample by the beam of electron is normally in the pattern of raster scan. The image of the sample that is produces, when the detected signal is combined with the position of beam of electron.
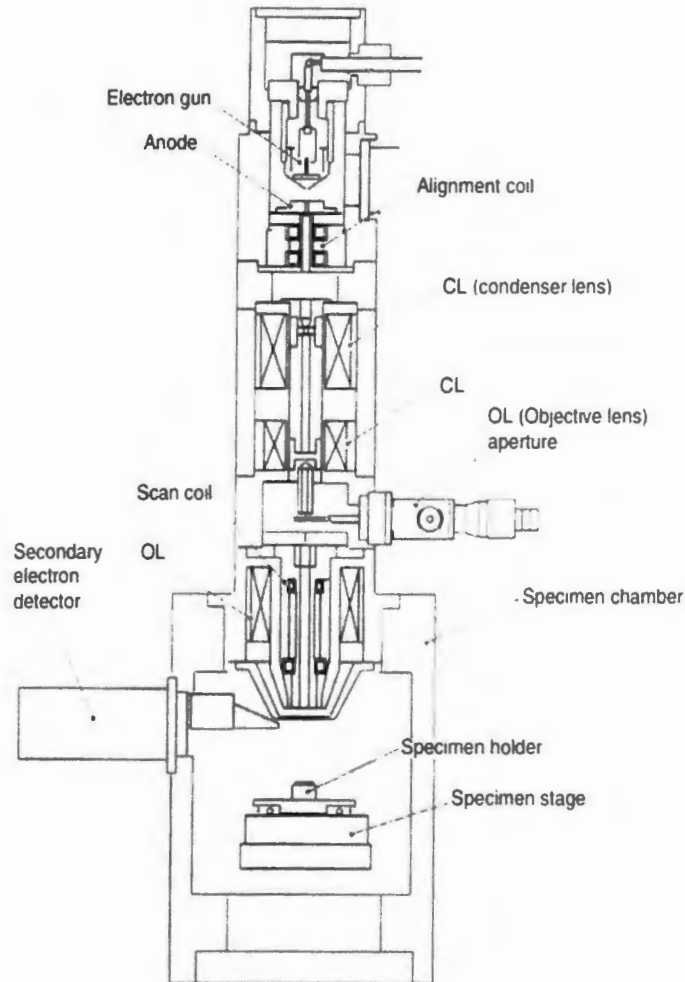
Fig 3.8: Schematic diagram of SEM various parts.

3.7.1 Components of SEM

- **Electron Gun**

    The electron gun is responsible for emitting electron beams which are striking on the surface of the sample to detect their properties like surface topography and the composition of the sample.

- **First Condenser lens**

    The first condenser lens is responsible for focusing the electron beams emitted by the electron gun to the second condenser lens.

- **Second Condenser lens**

     The second condenser lens is also called the objective lens. It is responsible for the size of the beam of electron impinging on the surface of the sample.

- **Deflection Coils**

     The electromagnetic deflection coils are responsible due to the deflection of the beam of electron for moving the scanning of the raster scan pattern.

- **Detectors**

     The collection and measurement of secondary electrons and back scattered electrons are combined by transducers or detectors. The detectors are doped glass or incident plastic material. When electrons strike on the detectors visible photons are emitted. Due to this process, the generation of electron-hole pairs will occurre. So, the conductivity is increased.

3.7.2 Working principle of SEM

     The electrons emitted by the electron gun are interacted with the sample atoms. This focused beam of electrons generating many signals like secondary electrons (SE), back-scattered electrons (BSE) and characteristic X-rays. These signals produced by scanning electron microscope (SEM) have information about the composition and the sample's surface topography.

     In scanning electron microscope (SEM), the electrons produced in the form of ionization products with relatively high energy are called secondary electrons (SE) because the secondary electrons are produced by the primary radiation (i.e. the beam of electrons emitted by the electron gun). With the help of secondary electron imaging (SEI), the images of very high resolution of a surface of a sample can be produced.

     The beam of electrons strikes on the surface of the sample and then reflected back from the sample due to the elastic scattering of electrons, called back-scattered electrons (BSE). Due to the strong relationship between the signal intensity of back-scattered electrons (BSE) and the sample's atomic number (Z), the images of the sample can be produced from back-scattered electrons (BSE) which give details about the mixing of different elements.

     When the electron of inner shell is removed from the specimen by the beam of electron, the characteristic X-rays are emitted. This is due to the inner shell is completed by the electron of high energy. By using this signal to detect the composition of the specimen and calculate the population of elements in the specimen.

3.8   Resistivity measurements by Four-probe method

To calculate the critical temperature 'T_c' of the super-conductor (i.e. resistance is equal to zero, R=0) by using measure the resistivity of a super-conductor. In normal state, the electrons scattering due to the defects in lattices, the vibrations of atoms in the lattice and the collisions between the electrons are the resistivity sources of the conducting materials [61].

The simple approach is used for the measurements of the resistivity of conducting materials is the four-probe method. The surface of the rectangular shaped sample is connected by the four probes. Low resistance contacts are normally used to connect the probes to the surface of the sample. The formula for the measurements of the resistivity is,

$$\rho = \frac{V(T)A}{IL}$$

Where, V(T) is the drop of the voltage across the surface of the sample. 'L' is the sample's length. 'I' is the current flow through the surface of the sample and 'A' is the sample's area of cross-section.

The current supply to the sample by a source of constant current across the outer probes and measure the voltage between the middle probes. During measurements apply a current of few mille-amperes (such as 1 or 2mA). The resistivity vs temperature is measured by using a liquid nitrogen dower which acts as a cryostat. During the cycle of heating such as 77K reaches to the room temperature, so we get the measurements about resistivity. Now, the data is record by using the resistivity measurements setup as shown in fig: 3.9.
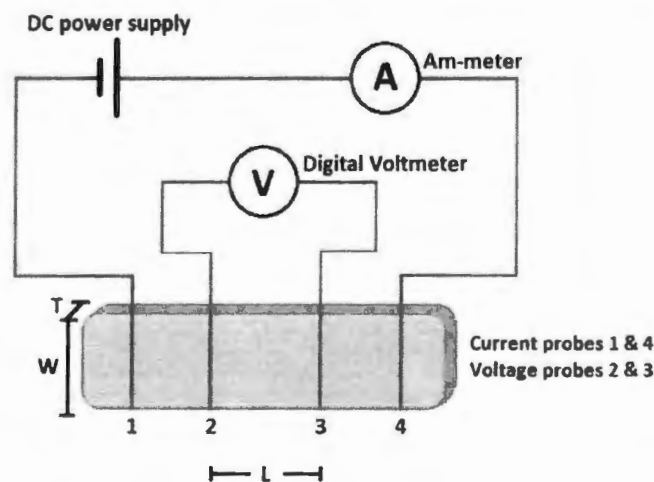
Fig 3.9 Four point probe mechanism for RT-measurements.

3.9 Dielectric Measurements by LCR Meter

We can find dielectric measurements of the materials by using LCR meter. Our study is also about the dielectric measurements of the materials, so we use LCR meter to find dielectric properties of $(Co_3O_4)_x$/CuTl-1223. Several steps are involving to find dielectric measurements of the material.

First step is the conducting layers are made on the side of the sample. These conducting layers are made of silver paste. Between these conducting layers the sample acts as an insulating material. Now these conducting layers are fixed with the sample holder. This part of sample holder contains thermocouple. Now these silver pasted conducting layers are attached to the silver pasted electric cables. Then, connect with LCR meter and the thermocouple is connected to the P-2000/E KEITHLEY MULTIMETER. By using these connections we find out the temperature in terms of voltage. The point thermocouple is connected with conducting layers is dropped into the liquid nitrogen [62]. The metallic cap is used to cover the sample holder and controlling the sample's temperature by dropping and raising the junction point into the liquid nitrogen. Different readings of dielectric measurements of the sample are recorded on the LCR meter

Fig 3.10: LCR meter

Chapter No. 4   Results and discussion

4.1   X-Ray diffraction (XRD) analysis

X-ray diffraction peaks of Co_3O_4 nanoparticles are shown in fig. 4.1. Various planes like (0 2 2), (1 1 3), (0 0 4), (1 3 3), (2 2 4),(3 3 3),(0 0 4),(0 0 6) and (3 3 5) are indexed according to the face centered cubic crystal structure (space group *Fd3m*) corresponding to different 2θ values such as 31.25^o, 36.91^o, 44.92^o, 49.16^o , 55.74^o , 59.44^o , 65.41^o , 69.31^o and 77.35^o respectively. Debye-Scherer formula was used to find the average crystallite size of Co_3O_4 nanoparticles and was found to 71 nm. Most of the diffraction peaks are well matched according to face centered cubic crystal structure of Co_3O_4 nanoparticles without any traces of other phases or impurities [64].
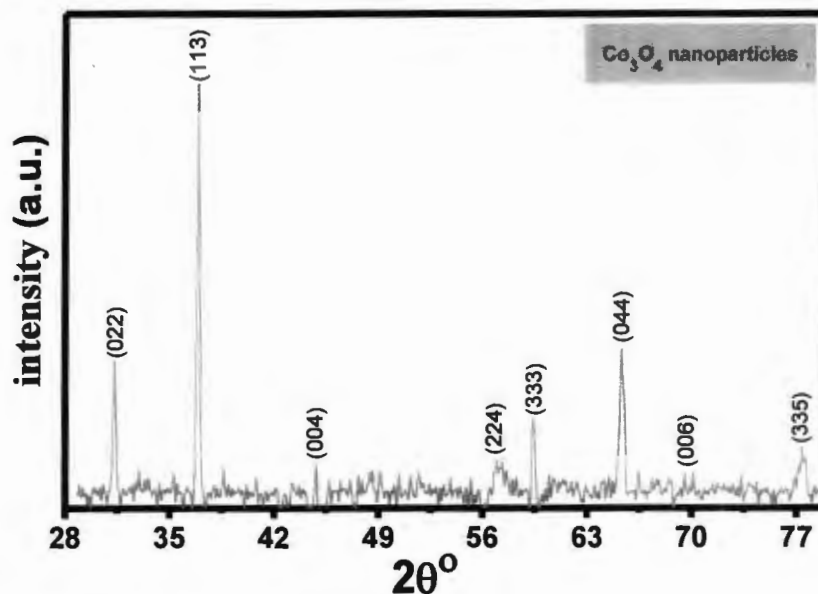
Fig4.1: XRD pattern of Co_3O_4 nanoparticles.

XRD spectra of $(Co_3O_4)_x$/CuTl-1223 nanoparticles-superconductor composites with x = 0, 1.0 wt.% are shows in fig. 4.2. These diffraction spectra demonstrate the predominance of CuTl-1223 superconducting phase, as the majority of the diffraction peaks have been all around coordinated agreeing the tetragonal structure of this phase by taking after p4/mmm space gathering. The structure of host CuTl-1223 superconducting phase was unaltered after the addition of these Co_3O_4 nanoparticles. These diffraction peaks accommodated that the structure of host CuTl-1223 superconducting phase stayed unaltered by the addition of Co_3O_4 nanoparticles, which shows that occupancy of these nanoparticles at grain-boundaries. Few un-indexed diffraction peaks of low intensity because of some other superconducting phases and impurities. [63].
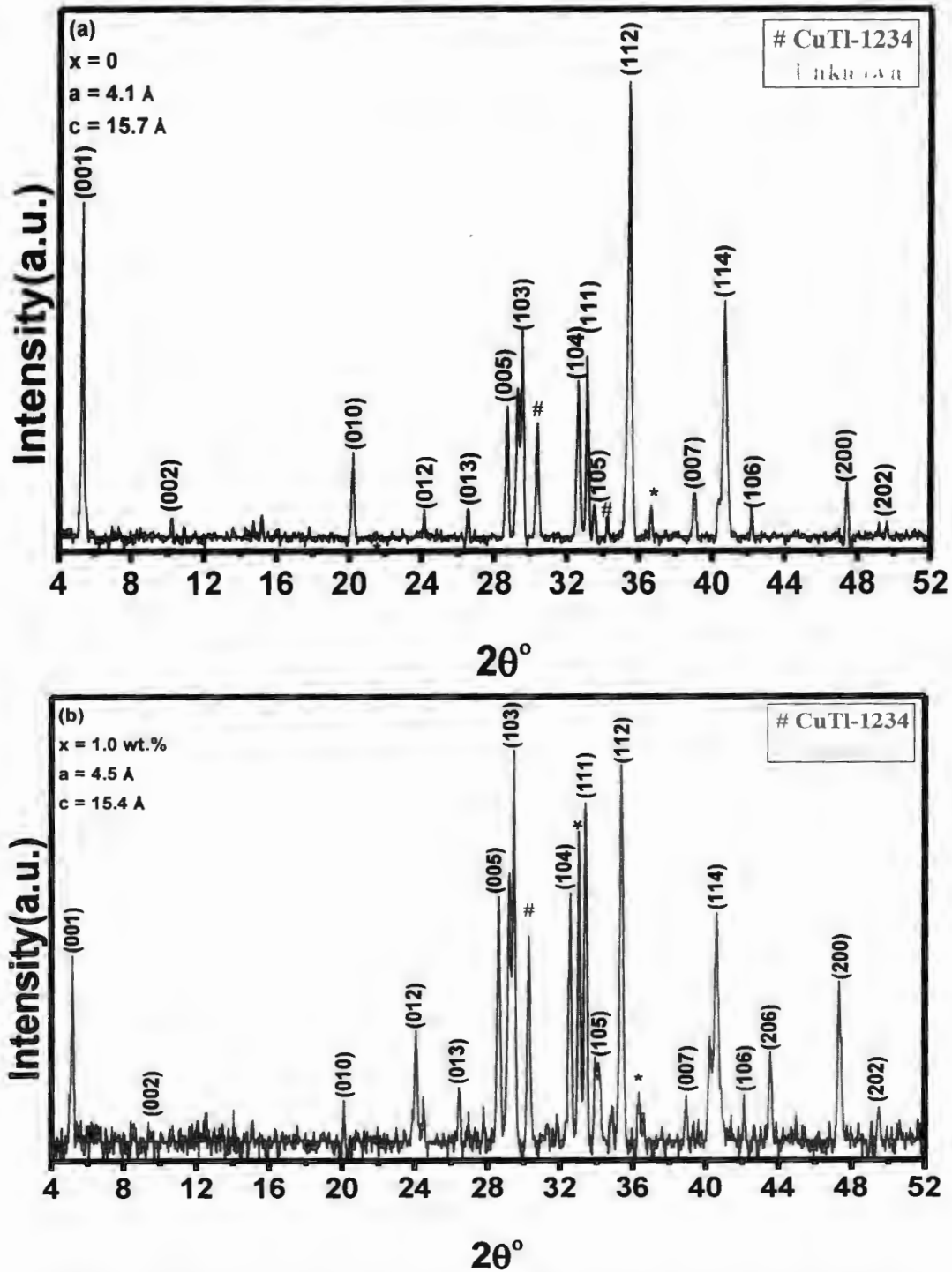
Fig4.1: XRD of $(Co_3O_4)_x$/CuTl-1223 composites with(a) x=0 and (b) x=1.0wt.%

4.2   Resistivity measurement

The dc-resistivity versus temperature (R-T) measurements of $(Co_3O_4)_x$/CuTl-1223 with x = 0, 1.0 and 1.0 wt. % is shown in Fig. 4.3. These measurements show metallic

variation from 300 K down to onset of superconductivity for all these samples. The value of (T_c^{onset}) was found around 105 K for un-added nanoparticle in the sample and then decreased to 40 K with the increasing concentration of these Co_3O_4 nanoparticles up to 2.0 wt. %. The decreased in T_c^{onset}(K) with Co_3O_4 nanoparticles addition in CuTl-1223 phase, is most probably due to presences of these semiconducting nature of nanoparticles across grain-boundaries may causes the break-up of cooper pairs and enhanced the scattering cross-section of carriers [65].
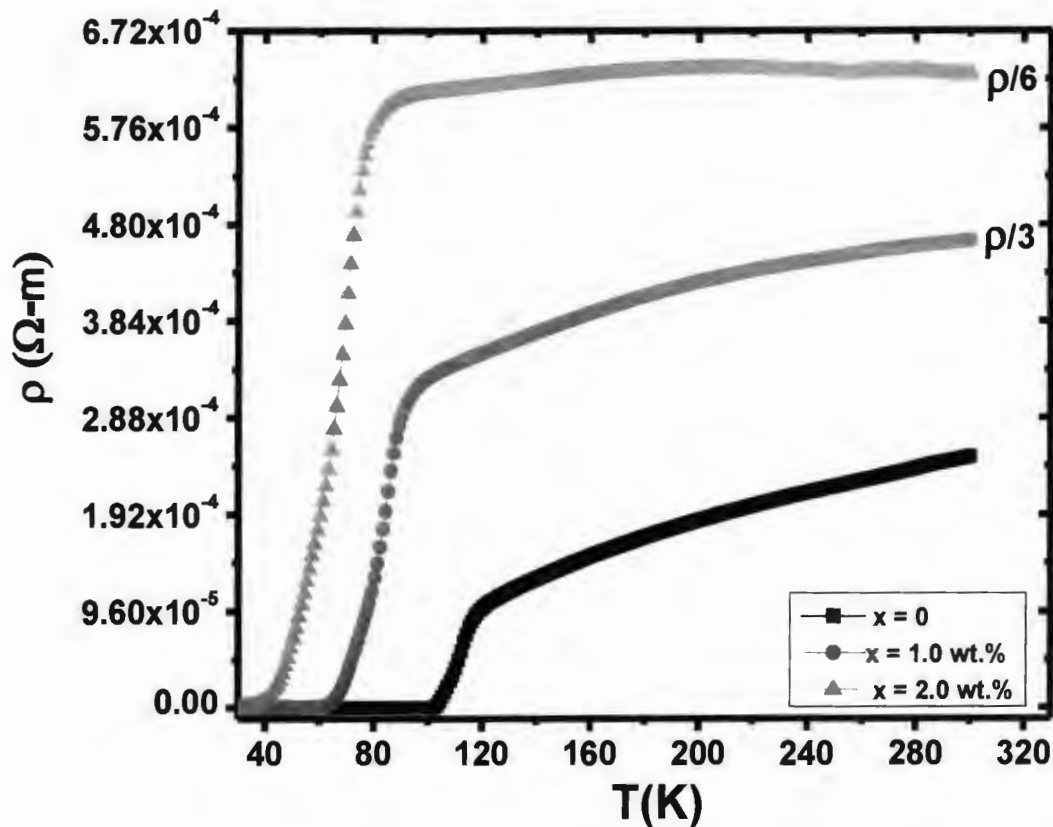
Fig.4.3: Resistivity vs temperature measurements of $(Co_3O_4)_x$/CuTl-1223 superconductor composite with x =0, 1.0 and 2.0 wt.

4.3   Dielectric analysis

4.3.1 Real part of dielectric constant (ε'_r)

We have studied the dielectric properties of $(Co_3O_4)_x$/(CuTl-1223) nanoparticles-superconductor composites with x = 0, 0.5, 1.0, 2.0 wt. %. We calculated the complex

dielectric constants ($\varepsilon_r = \varepsilon'_r + \varepsilon''_r$) and absolute dielectric loss tangent (tan δ) and ac-conductivity by experimentally measuring the capacitance (C) and conductance (G) at frequency ranges 40 Hz to 100 MHz at various operating temperatures from 78 to 298 K with the aid of LCR meter. The capacitance, conductance, complex dielectric constant, and dielectric loss and ac-conductivity are the main parameters for the selection of the material as a dielectric for device applications. We used following expressions to calculate these parameters are express [66-70].

$$\varepsilon'_r = Cd/\varepsilon_0 A$$

The dielectric response of cuprates and ferrites can be explained by Koop's theoretical model. Koop's model is considered as a two layer model with grains (conducting region) and grains-boundaries (resistive region). The charge carriers faced hurdle to flow from grains (conducting region) to grain-boundaries (non-conducting region) and impurity atoms segregate along these grain-boundaries due to their higher energy state. When electric field is applied to the sample, then a portion of energy stored within the sample due to applied field is known as real part of the dielectric constant (ε'_r). The real part of dielectric constant of $(Co_3O_4)_x/(CuTl-1223)$ nanoparticles-superconducting matrix with x = 0, 0.5, 1.0, 2.0 wt. % at frequency ranges from 40 Hz to 100 MHz at different temperatures (78 to 298 K) are shown in Fig 4.4(a-d). At lower frequency of 40 Hz, high value of ε'_r has been observed in all the samples which correspond to Max Wegner effect [71-74]. This is probably due to space charge polarization in inhomogeneous dielectric material. The maximum values of ε'_r at frequency of 40 Hz and at 78 K temperature were found around 1.258×10^4, 4.258×10^3, 3.9×10^3, and 3.13×10^4 for the samples with x = 0, 0.5, 1.0 and 2.0 wt. %, respectively. By the inclusion of Co_3O_4 nanoparticles in CuTl-1223 matrix, overall decreasing trend was observed, which is due to semiconducting nature of these Co_3O_4 nanoparticles.

These semiconducting nature Co_3O_4 nanoparticles were settled at grain-boundaries and improve the inter-grains weak links which results in the reduction of oxygen vacancies and enhancement of charge carries at grain-boundaries. In the inset of fig. 4.4 (a-d), the variation of ε'_r versus temperatures at low frequency of 40 Hz is shown. The maximum values of ε'_r at frequency of 40 Hz varied from 9.03×10^3 to 1.25×10^4, 2.15×10^3 to 4.26×10^3, 1.7×103 to 3.91×10^3 and 1.8×10^3 to 3.1×10^3 at 78 K to 298 K for sample x = 0, 0.5, 1.0 and 2.0 wt. % respectively. It means that by increasing temperatures from superconducting state to normal

state the real part of dielectric constant ε'_r has been increased for all the samples which probably due to increasing polarizability of the material [75-77].
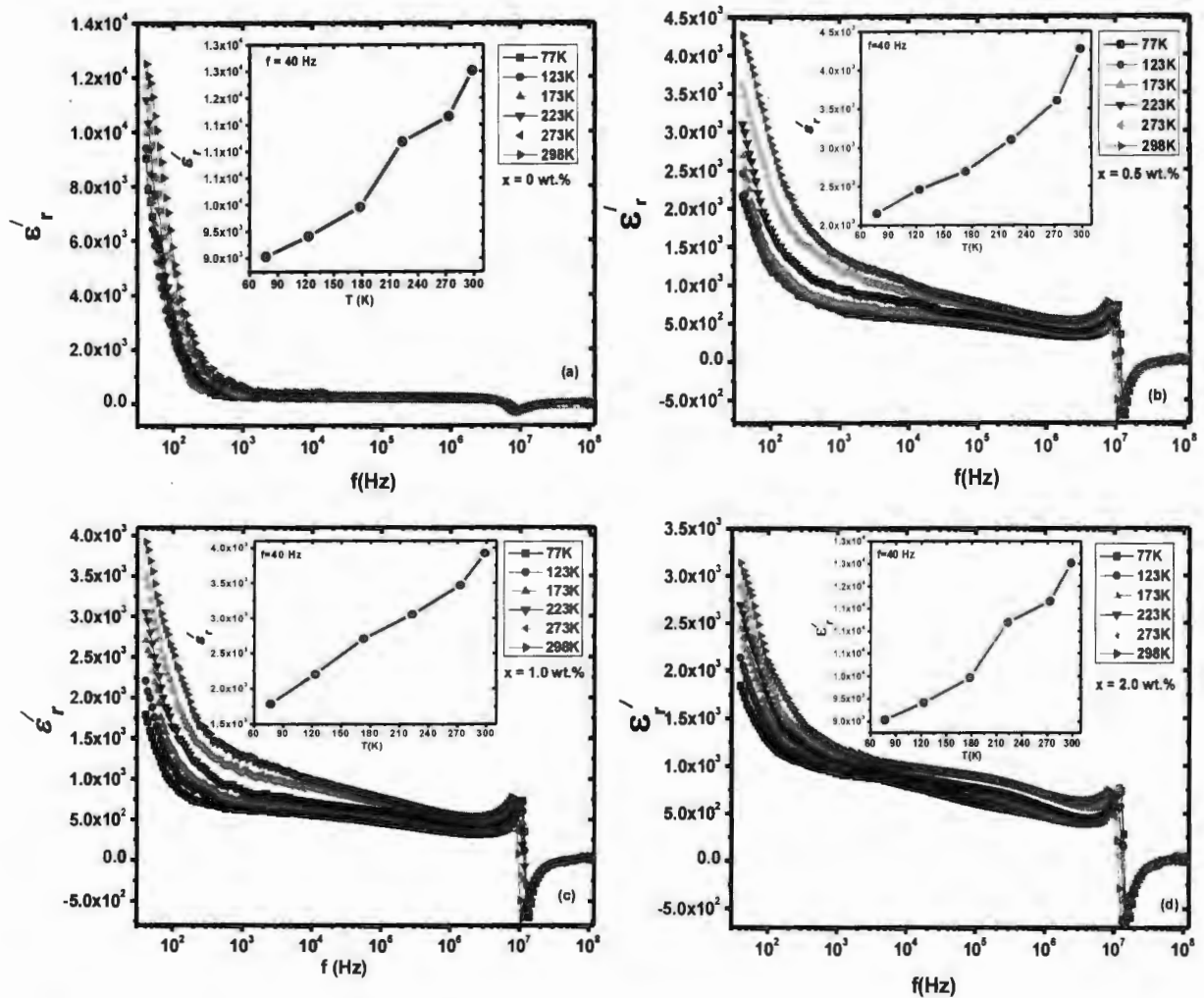
Fig.4.4 (a-d): The variation in real part ε'_r verses frequency of $(Co_3O_4)_x$/CuTl-1223 nanoparticle -superconductor for (a) x =0,(b) x = 0.5,(c) x =1.0 and (d) x =2.0 wt% at T = 78 K to 298 K. The variation of ε'_r vs temperatures are shown in the insets.

4.3.2 Imaginary part of dielectric constant (ε''_r)

When material is exposed to ac electric field then the amount of energy absorbed and attenuate is known as imaginary part ε''_r [78-81]. The mathematical expression for ε''_r is

$$\varepsilon''_r = Gd/\varepsilon_o A\omega$$

The change in value of imaginary part as a function of temperature (77 K to 298 K) and frequency range from (40 Hz to 100 MHz) is observed for $(Co_3O_4)_x$/CuTl-1223 superconducting composites with different concentration of Co_3O_4 nanoparticles are shown in

Fig. 4.5. At T= 78 K and frequency of 40 Hz value of ε''_r are calculated as 3.3×10^7, 3.07×10^6, 1.56×10^6 and 6.9×10^5 for the samples (x = 0 to 2.0 wt.%) respectively. It is found that the value of ε''_r suppressed by the addition of these Co_3O_4 nanoparticles, which is due to the semi-conducting nature of these nanoparticles. These nanoparticles enhanced the charge carriers which result in reduction of barriers that are responsible for polarization in the sample. In the inset of fig. 4.4
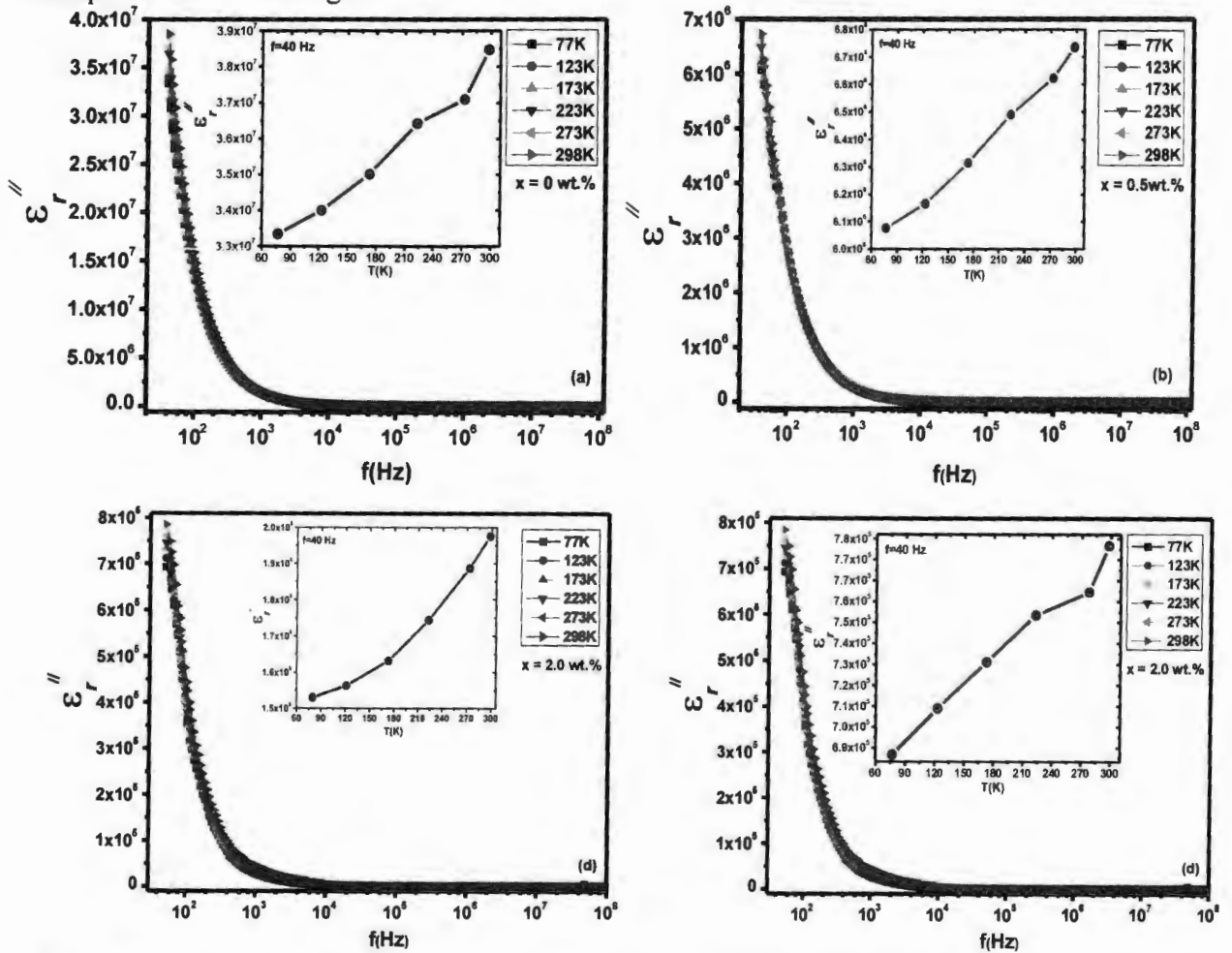
Fig. 4.4(a-d): The variation in imaginary part ε''_r verses frequency of$(Co_3O_4)_x$/CuTl-1223composite for (a) x =0,(b) x = 0.5,(c) x =1.0 and (d) x =2.0 wt% at T = 78 K to 298 K. The variation of imaginary part vs temperatures are shown in the insets.

ε''_r with operating temperature at low frequency of 40 Hz are shown. The values are found around 3.3×10^7 to 3.8×10^7 , 6.07×10^6 to 6.73×10^6 , 1.56×10^6 to 1.9×10^6 and 6.9×10^5 to 7.8×10^5 for x = 0, 0.5, 1.0, ,and 2.0 respectively. This increase in ε''_r with increasing temperature for all the samples is due to the enhancement of polarization in the material. At low frequency a high value of ε''_r was observed then start decreasing and almost constant at high frequency. This is because at low frequency the material can easily respond

to electric field. This can also be explained with the help of Maxwell Wagner model and Koop's theory, which is already mentioned above in real part.

4.3.3 Dielectric loss tangent (tan δ)

The ratio of energy attenuation (imaginary part) and energy absorbed (real part) is known as tangent loss (tan δ). The expression for tangent loss is given below

$$\tan \delta = \varepsilon''_r / \varepsilon'_r$$

The value of tan δ loss of $(Co_3O_4)_x$/CuTl-1223 nano-superconductor with (x = 0.0 to 2.0 wt.%) by varying both frequency (40 Hz to 100 MHz) and temperatures (78 K to 298 K) are shown in Fig. 4.6.
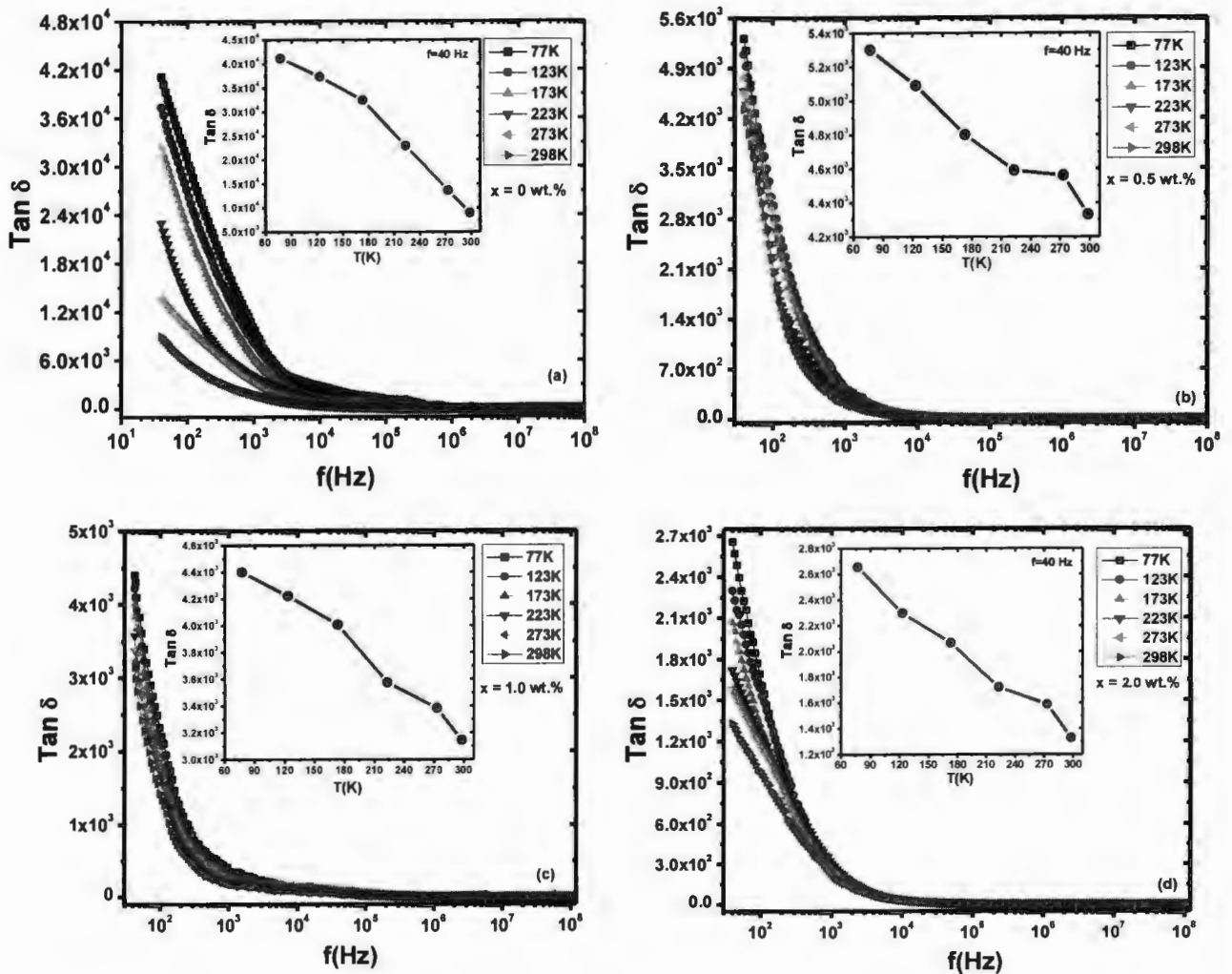
Fig.4.6: The variation in tangent loss of dielectric verses frequency of (Co_3O_4)x/CuTl-1223 composite with x =0, 0.5, 1.0 and 2.0 wt% at T = 78 K to 298 K. The variation of

tangent loss vs operating temperatures is shown in the insets.

At low frequency of 40 Hz and 78 K temperatures the calculated values of tangent loss for x = 0, 0.5, 1.0 to 2.0 wt.% of added nanoparticles in this phase were found around 4.1×10^4, 5.3×10^3, 2.5×10^3 and 2.6×10^3 respectively. The decreasing trend in all the samples was observed, this is because of semiconducting nature of these nanoparticles across grain-boundaries [82-83]. In the same way inset graph exhibits variation in tan δ loss at temperature ranges 78 K~ 278K are 4.1×10^4 to 8.9×10^3, 5.3×10^3 to 4.3×10^3, 2.5×10^3 to 1.3×10^3 and 2.6×10^3 to 1.3×10^3 for different concentrations of nanoparticles. Inset graph shows the value of tan δ loss decreasing with rise in temperature from 78 K~ 278K, which is due to polarization mechanism in the system.

4.3.4 AC conductivity (σ_{ac})

The ac-conductivity (σ_{ac}) of $(Co_3O_4)_x$/CuTl-1223 (x = 0, 0.5 1.0, and 2.0 wt.%) nanoparticles-superconductor composites at operating temperatures from 78 K to 298 K with test frequency ranges from 40 Hz to 100 MHz are shown in Fig. 7(a-d). The value of σ_{ac} at lower frequency of 40 Hz were found around 7.38×10^{-5}, 3.2×10^{-4}, 3.35×10^{-4} and 5.56×10^{-4} at 78 K temperature for the samples with x = 0 to 2.0 wt. %, respectively. It is found that by the addition of Co_3O_4 nanoparticles σ_{ac} of the material increases which is due to the semiconducting behavior of these nanoparticles across grain-boundaries. These Co_3O_4 nanoparticles were settled at grain-boundaries and improve the pores and voids which results and enhancement of charges by the reduction of oxygen vacancies which result in increasing conductivity of CuTl-1223 matrix. In the insets of fig. 7(a-d),
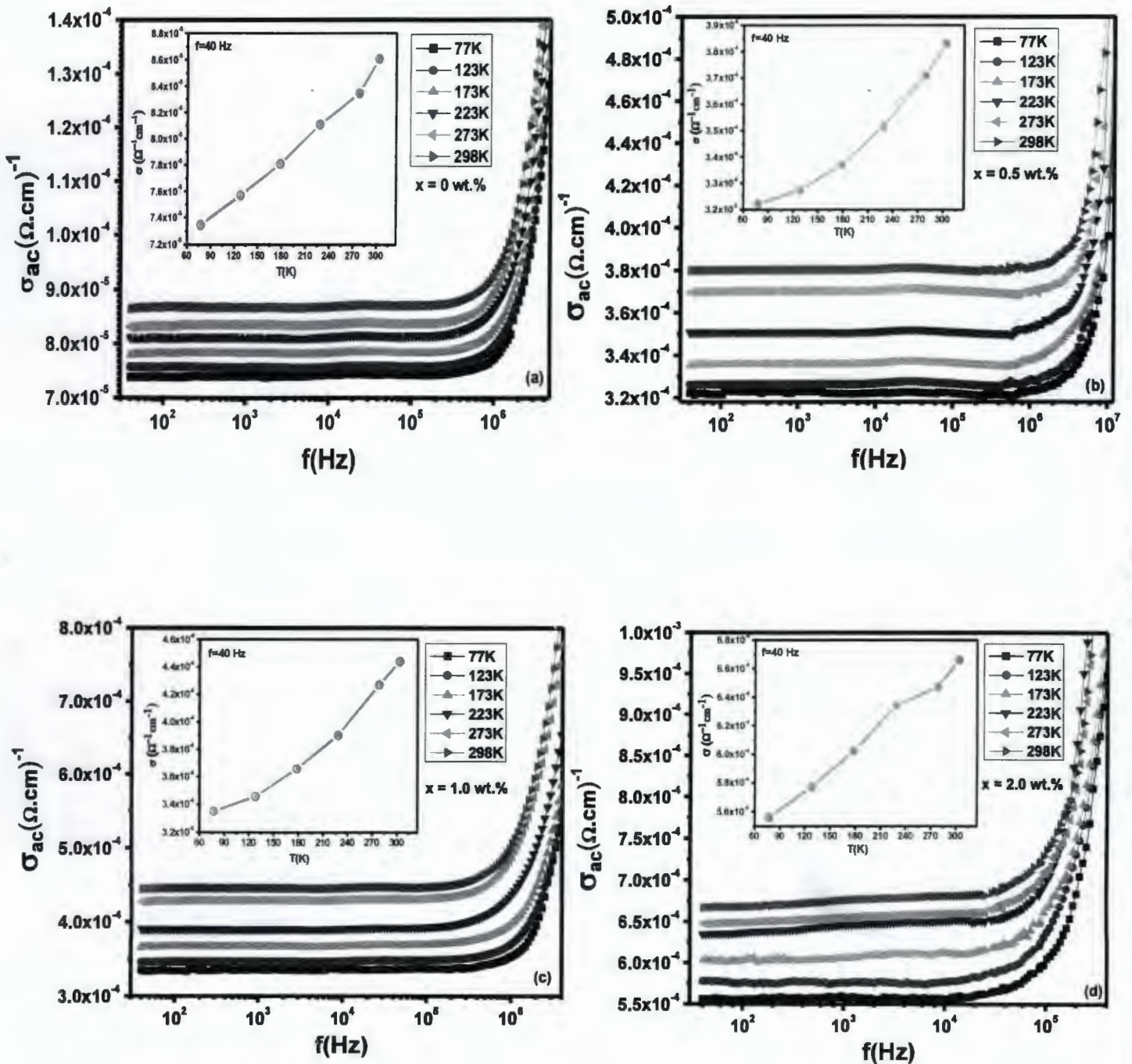
Fig.4.7: The variation in ac-conductivity of verses frequency of$(Co_3O_4)_x$/CuTl-1223compositewithx =0, 0.5, 1.0 and2.0 wt% at T = 78 K to 298 K. The variation of ac-conductivity vs temperatures at 40 Hz frequency is shown in the insets.

the variation of σ_{ac} versus operating temperatures at low frequency of 40 Hz is shown. The value of σ_{ac} at lower frequency of 40 Hz varied from 7.38×10^{-5} to 8.64×10^{-5}, 3.2×10^{-4} to 3.79×10^{-4}, 3.35×10^{-4} to 4.4×10^{-4} and 5.56×10^{-4} to 6.6×10^{-4} at temperatures 78 K to 298 K for x = 0, 0.5, 1.0 and 2.0 wt. % added nanoparticles in host matrix, respectively. This is attributed to the gradual increase in σ_{ac} with increasing value of operating temperatures, which is due to the release of space charges and enhancement in hopping rate of mobile charge carriers with the suppress of non-stoichiometric distribution of oxygen vacancies and dangling bonds at grain-boundaries [84-85]

Conclusion

After successfully synthesized CuTl-1223 phase by solid state reaction method, we tuned the superconducting and dielectric properties of $(Co_3O_4)_x/(CuTl-1223)$ superconducting composites with x = 0, 0.5, 1.0 and 2.0 wt. %. XRD revealed that no alteration in the tetragonal crystal structure of bulk CuTl-1223 matrix after the inclusion of Co_3O_4 nanoparticles. The decrease in superconducting properties is due to breaking mechanism and scattering of carriers across these nanoparticles. In order to investigate the dielectric properties we used different parameters such as by varying frequency at operating temperatures (78K to 298K) and varying the contents of Co_3O_4 nanoparticles (x= 0 to 2 wt.%). A high value of dielectric constant was observed at low frequency which is due to the slow response of mobility with applied frequency. The overall suppress in both real and imaginary parts of dielectric constant have been observed in all samples, which is attributed to semiconducting nature Co_3O_4 nanoparticles. By increasing temperature both real and imaginary part of dielectric constant increases and tangent loss decreases which is probably due to the enhancement of polarizability in $(Co_3O_4)_x/(CuTl-1223)$ composites. The increase in conductivity of the material was observed, which is due to the semiconducting nature of nanoparticles enhanced the carrier's concentration and reduce the oxygen vacancies at grain-boundaries.

[19] N. Kobayashi, H. Iwasaki, S. Terada, K. Noto, A. Tokiwa, M. Kikuchi, Y. Syono, and Y.Muto,PhysicaC,**1525**,155(1988).

[20] T.Worthington,W. J. Gallagher, and T. R. Dinger, Phys. Rev. Lett. **59**,1160(1987).

[21] A. Schilling, O. Jeandupeux, S. Buchi, H. Ott and C. Rossel, Physica C, **229**,240 (1994).

[22] M. J. Rice and Y. R. Wang, Phys. Rev. **B37**, 5893 (1988).

[23] J. Carini, L. Drabeck, and G. Gr ̈uner, Mod. Phys. Lett. **B3**,5(1989).

[24]A. J. Mestel, "Magnetic levitation of liquid metals" J. Fluid. Mech. **117**, 27 (1982).

[24] C. N. R. Rao, A. Muller, and A. K. Cheetam, "The Chemistry of Nanomaterials: Synthesis Properties and Applications" Wiley-VCH, Weinheim, pp. 20–30 (2004).

[25] P. D. C. Burda, "Metallic Nanomaterials" J. Am. Chem. Soc. **131**, 6642 (2009).

[26] Y. Li, X. Fan, J. Qi, J. Ji, S. Wang, G. Zhang, and F. Zhang, "Gold nanoparticles graphene hybrids as active catalysts for Suzuki reaction" Mater. Res. Bull. **45**, 1413 (2010).

[27] G. Schmid, and B. Corain, "Nanoparticulated gold: syntheses, structures, electronics, and reactivities" Eur. J. Inorg. Chem, **2003**, 3081 (2003).

[28] A. K. Gupta, and M. Gupta, "Synthesis and surface engineering of iron oxide nanoparticles for biomedical applications" Biomater. **26**, 3995 (2005).

[29] V. Radmilovic, "Advanced imaging and biomedical applications of nanomaterials", J. Serb. Soc. Comput. Mech. **5**, 24 (2011).

[30] I. R. Bunghez, M. E. BarbintaPatrascu, N. Badea, S. M. Doncea, A. Popescu, and R. M. Ion, "Antioxidant silver nanoparticles green synthesized using ornamental plants" J. Optoelect. Adv. Mater. **14**, 1016 (2012).

[31] H. Naceur, A. Megriche, and M. E. Maaoui, "Frequency-dependant dielectric characteristics and conductivity behavior of $Sr_{1-x}(Na_{0.5}Bi_{0.5})_xBi_2Nb_2O_9$ (x = 0.0, 0.2, 0.5, 0.8 and 1.0) ceramics" Orient. J. Chem. **29**, 937 (2013).

[32] S. Cavdar, H. Koralay, N. Tugluoglu, and A. Gunen, "Frequency-dependent dielectric characteristics of Tl–Ba–Ca–Cu–O bulk superconductor" Supercond. Sci. Technol. **18**, 1204 (2005).

[33] L. F. Chen, C. K. Ong, C. P. Neo, V. V. Varadan, and V. K. Varadan, "Microwave Electronics" Wiley Blackwell (2004).

[34] S.Çavdar, Ş., H. Koralay, N. Tuğluoğlu, and A. Günen. "Frequency-dependent dielectric characteristics of Tl–Ba–Ca–Cu–O bulk superconductor."*Superconductor*Science and Technology **9**, 1204 (2005).

[35] Aly, A. Abou, N. H. Mohammed, R. Awad, H. A. Motaweh, and D. El-Said Bakeer. "Determination of superconducting parameters of $GdBa_2Cu_3O_{7-\delta}$ added with nanosized ferrite $CoFe_2O_4$ from excess conductivity analysis. "Journal of superconductivity and novel magnetism 25,2281(2012).

[36]. E. T. Koparan, M. M. Hassan, A. Surdu, K. Kizilkaya, A. Sidorenko, and E. Yanmaz, "Pinning enhancement in MgB2 superconducting thin films by magnetic nanoparticles ZnO" Bull. Mater.Sci. 36, 961 (2013).

[37] H.A Hashem and S.Abouelhassan, ''dielectric properties of SnSthin film'' Chinese Journal of Physics ,43,955(2005).

[38] H. Koraly and S. Altındal "Effect of vanadium substitution on the dielectric properties of glass ceramic Bi-2212 superconductor" J. Low Temp. Phys. 164,102,(2011).

[39] N. A. Khan, M. Mumtaz, and A. A. Khurram. "Frequency dependent dielectric properties of $Cu_{0.5}Tl_{0.5}Ba_2 Ca_2Cu_{3-y} Zn_yO_{10-\delta}$ (y= 0, 1.0, 1.5, 2.0, 2.5) superconductors." *J. Applied Phys.* 104,033916 (2008).

[40] M .Mumtaz, M. Kamran, K. Nadeem, A. Jabbar, N.A. Khan, A.Saleem, S. T. Hussain, and M. Kamran. " Dielectric properties of (CuO, CaO_2, and BaO) y/CuTl-1223 composites." Low Temperature Physics 39,622 (2013).

[41] Yimin Cuy, N. Lih Wu, Y. Der Yao, S. Nan Lee, S. Yen Wong, and E. Ruckenstein, "Synthesis ofTl2CanBa2Cun+1O6+2n (n=1, 2) from stoichiometric reactant mixtures" Physica C.161,302,(1989)

[42] Ilyushechkin, Alexander Y., Igor E. Agranovski, Igor S. Altman, and Mansoo Choi. "Effect of MgO nanoparticles embedded into Bi-2212/Ag tapes on the microstructure and superconducting properties." Materials Science and Engineering B 167, 60 (2010).

[43]M. Farbod ,L. Raffo, R. Cacioffu, D. Rinaldi, and F. Licci, Supercond. Sci. Technol. 8, 409, (1995).

[44]M. Mumtaz, M. Kamran, K. Nadeem, A. Jabbar, Nawazish A. Khan, A. Saleem, S. TajammulHussain, and M. Kamran, "Dielectric properties of (CuO,CaO2, and BaO)y/CuTl-1223 composites" Low Temp. Phys. 39, 136 (2013).

[45]M. Mumtaz, M. Kamran, K. Nadeem, A. Jabbar,N. A. Khan, A. Saleem, S. Tajammul. Hussain, and M. Kamran, "Dielectric properties of (CuO,CaO2, and BaO)y/CuTl-1223 composites" Low Temp. Phys. 39,136 (2013).

[76] M. Mumtaz, M. Rahim, N. A. Khan, K. Nadeem, and K. Shehzad, "Dielectric properties of oxygen post-annealed $Cu_{0.5}Tl_{0.5}Ba_2Ca_3(Cu_{4-y}Cd_y)O_{12-\delta}$ bulk superconductor" Ceram. Int. **39**, 9591 (2013).

[77] M. Rahim, N. A. Khan, and M. Mumtaz, "Temperature and frequency dependent dielectric properties of $Cu_{0.5}Tl_{0.5}Ba_2Ca_3(Cu_{4-y}Cd_y)O_{12-\delta}$ bulk superconductor" J. Low Temp. Phys. **172**, 47 (2013).

[78] X. Xu, Z. Jiao, M. Fu, L. Feng, K. Xu, R. Zuo, and X. Chen, "Dielectric studies in a layered Ba based Bi-2222 cuprate $Bi_2Ba_2Nd_{1.6}Ce_{0.4}Cu_2O_{10+\delta}$" Physica C **417**, 166 (2005).

[79] S. F. Mansour, "Frequency and composition dependence on the dielectric properties for Mg-Zn ferrite" Egypt. J. Solids **28**, 263 (2005).

[80]J. Yu, S. Tang, L. Zhai, Y. Shi, and Y. Du, "Synthesis and magnetic properties of single-crystalline $BaFe_{12}O_{19}$ nanoparticles" Physica B **404**, 4253 (2009).

[81] R.K. Kotnala, V. Verma, V. Pandey, V.P.S. Awana, R.P. Aloysius, and P.C. Kothari, "The effect of nano-SiO_2 on the magnetic and dielectric properties of lithium cadmium ferrite" Solid State Comm. **143**, 527 (2007).

[82] M. K. Fayek, M. K. Elnimr, F. Sayedahmed, S. S. Ata-Allah, and M. Kaiser, "Relaxation characteristics of $NiGa_xFe_{2-x}O_4$" Solid State Comm. **115**, 109 (2000)

[83] S. Suresh, "Synthesis, structural and dielectric properties of zinc sulfide nanoparticles" Int. J. Phys. Sci. **8**, 1121 (2013).

[84] M. Z. Ansar, S. Atiq, K. Alamgir, and S. Nadeem, "Frequency and temperature dependent dielectric response of Fe_3O_4 nano-crytallites", J. Sci. Res. **6**, 399 (2014).

[85] A. R. Shitre, V. B. Kawade, G. K. Bichile, and K. M. Jadhav, "X-ray diffraction and dielectric study of $Co_{1-x}Cd_xFe_{2-x}Cr_xO_4$ ferrite system",Mat. Lett. **56**, 188 (2002).